Synchronous Replication Initiation of Multiple Origins

Mareike Berger and Pieter Rein ten Wolde
Biochemical Networks Group, Department of Information in Matter, AMOLF, 1098 XG Amsterdam, Netherlands

(Received 3 April 2023; accepted 18 July 2023; published 8 August 2023)

Initiating replication synchronously at multiple origins of replication allows the bacterium *Escherichia coli* to divide even faster than the time it takes to replicate the entire chromosome in nutrient-rich environments. What mechanisms give rise to synchronous replication initiation remain, however, poorly understood. Via mathematical modeling, we identify four distinct synchronization regimes depending on two quantities: the duration of the so-called licensing period during which the initiation potential in the cell remains high after the first origin has fired and the duration of the blocking period during which already initiated origins remain blocked. For synchronous replication initiation, the licensing period must be long enough such that all origins can be initiated, but shorter than the blocking period to prevent reinitiation of origins that have already fired. Our model reveals that the delay between the firing of the first and the last origin scales with the coefficient of variation (CV) of the initiation volume. Matching these to the values measured experimentally shows that the firing rate must rise with the cell volume with an effective Hill coefficient that is at least 20; the probability that all origins fire before the blocking period is over is then at least 92%. Our analysis thus predicts that the low CV of the initiation volume is a consequence of synchronous replication initiation. Finally, we show that the previously presented molecular model for the regulation of replication initiation in *E. coli* can give rise to synchronous replication initiation for biologically realistic parameters.

DOI: 10.1103/PRXLife.1.013007

I. INTRODUCTION

Passing on the genetic information from one generation to the next with high fidelity is crucial for the survival of every organism. Many bacteria contain several copies of their chromosome [1–6]. In nutrient-rich environments, the bacterium *Escherichia coli* initiates DNA replication of several copies of the same chromosome synchronously with very high precision [2–4,7]. Already in the 1960s, Cooper and Helmstetter suggested that initiating new rounds of replication synchronously at several origins enables *E. coli* to divide even faster than the fixed time it takes to replicate its entire chromosome [8]: Rounds of replication that started in the mother cell continue to be replicated during cell division and finish only in the following generations [Fig. 1(a)]. To ensure that all daughter cells obtain a fully replicated copy of the chromosome at these high division times, replication must be initiated at all chromosomes synchronously. Later, Skarstad *et al.* confirmed the prediction of Cooper and Helmstetter by counting the numbers of origins in rapidly growing cultures: they found that most cells have 2^n $(n = 1, 2, 3)$ copies of their chromosome and only a small fraction of cells (2–7%) contained three, five, six, or seven chromosomes [9]. Recent single-cell measurements indeed show that *E. coli* initiates replication synchronously at up to eight origins with very high precision in the fast-growth regime [2,7]. It remains, however, an open question how *E. coli* achieves such a high degree of synchrony.

Replication initiation in *E. coli* is controlled by the initiator protein DnaA [10–13]. This protein can switch between two nucleotide-binding states, an inactive state in which DnaA is bound to ADP and an active one in which it is bound to ATP [2,13–17]. Both the inactive and active forms can bind to an origin of replication, but binding of the inactive state is not sufficient: replication initiation requires the binding of ATP-DnaA [12,18–20]. The evidence is accumulating that the origin binding of DnaA and hence replication initiation is controlled via two distinct mechanisms, titration and protein activation [13,17,21]. Titration of DnaA via high-affinity DnaA binding sites on the chromosome generates a cycle in the concentration of free DnaA that is available for binding to the origin [13,22], while an activation switch induces a cycle in the fraction of active DnaA [17,23,24]. These two cycles together conspire to generate robust oscillations in the concentration of free and active DnaA [25]. This concentration of free and active DnaA forms the initiation potential of the cell, which determines the propensity of origin firing.

Initiation synchrony entails that all origins are initiated during each cell cycle, yet also only once per cell cycle. This is a major challenge because the cell needs to meet two potentially conflicting constraints. The requirement that all origins must fire during each cell cycle means that when the first origin fires, the initiation potential cannot go down immediately: it must continue to rise so that also the other origins can fire. On the other hand, the origin that has fired should not fire again, even though the initiation potential is still rising. It appears that *E. coli* employs two distinct mechanisms to meet these two constraints. The oscillations in the

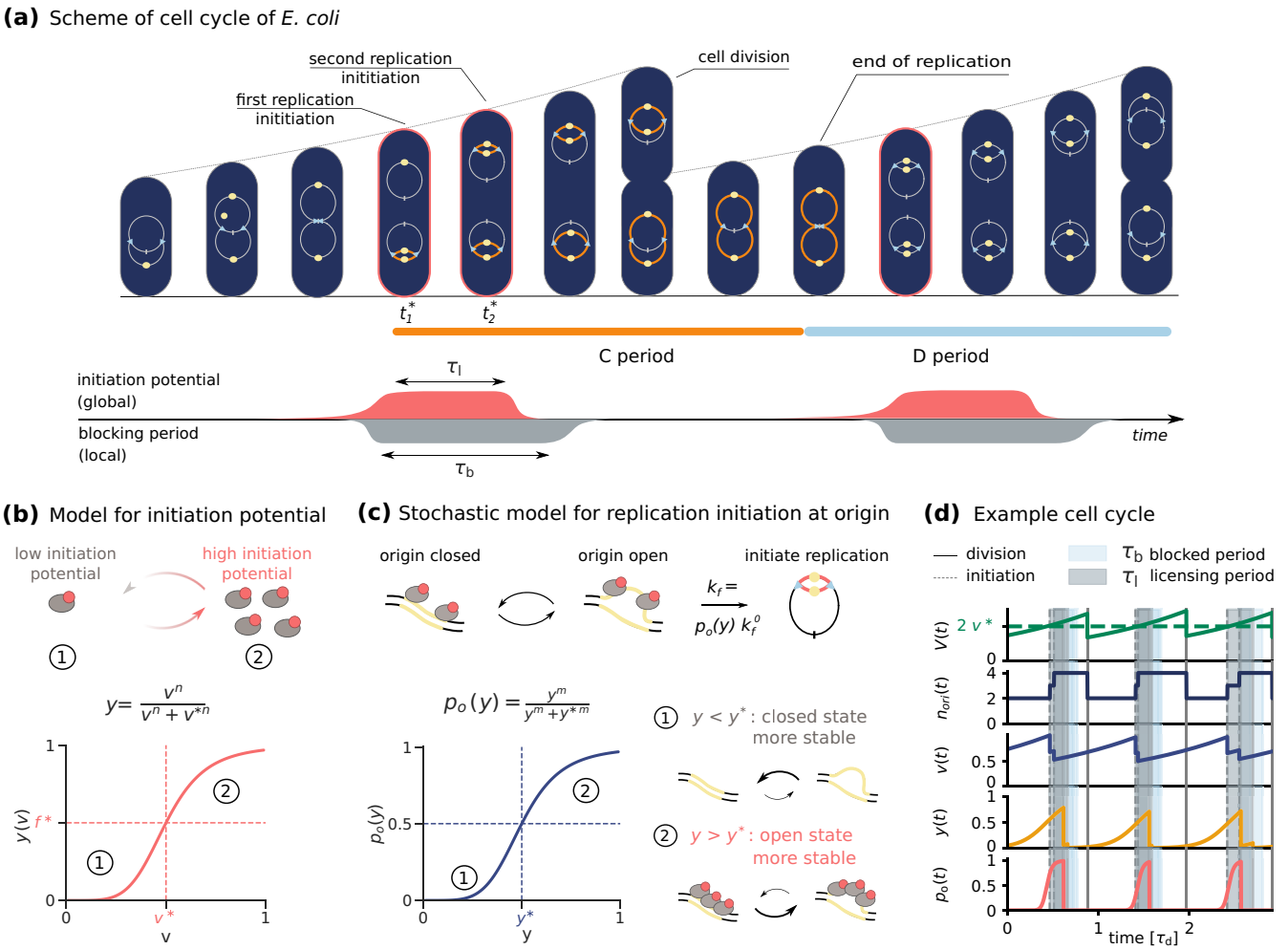

FIG. 1. Model of stochastic replication initiation at each origin. (a) Scheme of the cell cycle of *E. coli*: the volume of the cell grows exponentially with a growth rate λ. At doubling times $\tau_d = \ln(2)/\lambda$ that are shorter than the time to replicate the entire chromosome and divide (C+D period), cells are typically born with an ongoing round of chromosomal replication. Replication is initiated stochastically at each origin (yellow circles) at times t_1 and t_2, respectively, and the replication forks (blue triangles) advance towards the terminus (gray bar) with a constant replication speed. In *E. coli*, all origins fire within a very short time interval, thus giving rise to synchronous replication initiation. To fire replication synchronously a global and a local mechanism are required: the global mechanism keeps the initiation potential high for a licensing period τ_l (red shaded area), while the local mechanism based on SeqA prevents already initiated origins from refiring for a blocking period $\tau_b > \tau_l$ (gray shaded area). In our model, cell division is triggered a fixed cycling time $\tau_{cc} = T_C + T_D$ after replication has been initiated. (b) We model the initiation potential y in the cell as a function of the volume per origin, $v = V/n_{ori}$, via a Hill function with the Hill coefficient n. At the critical volume per origin, v^*, the initiation potential equals the critical initiation potential $y^* = 0.5$. (c) Stochastic model of replication initiation at the origin as a function of the initiation potential in the cell: the origin can be in an open or in a closed configuration and replication can be initiated with a constant rate k_f^0 if the origin is open. The probability to be in the open state $p_o(y)$ depends on the initiation potential in the cell and is modeled via a Hill function with the Hill coefficient m and the critical active fraction of DnaA, f^*. (d) The volume $V(t)$, the number of origins, $n_{ori}(t)$, the volume per number of origins, $v(t) = V(t)/n_{ori}(t)$, the initiation potential $y(t)$, and the opening probability $p_o(t)$ as a function of time (in units of the doubling time of the cell, τ_d). Every origin is initiated stochastically (dashed vertical gray lines) and during the blocking period τ_b (light blue shaded area) the newly replicated origins cannot be reinitiated. The initiation potential $y(t)$ and the opening probability $p_o(t)$ continue to increase during the licensing period τ_l (gray shaded area), such that the remaining origins that have not yet initiated replication are also initiated. At the end of the licensing period, the initiation potential $y(t)$ and therefore also the opening probability $p_o(t)$ instantaneously decrease to a lower value, making reinitiation highly unlikely. At cell division (vertical solid gray lines), the cell volume is divided by 2 and one of the two chromosomes is chosen at random for the next cell cycle. (See Table I for all parameters.)

initiation potential, the concentration of free and active DnaA, constitute a global mechanism that induces not only the first origin to fire, but also prompts, and allows, the remaining origins to fire [Fig. 1(a)]. To prevent the immediate reinitiation of origins that have already fired, a local mechanism is used.

The local mechanism that prevents the immediate reinitiation of newly replicated origins is based on the so-called sequestration of these origins. In *E. coli*, after an origin has initiated replication, the protein SeqA transiently binds to this origin and thus prevents that new rounds of replication start immediately again at the same origin [26,27]. When either

of the two proteins SeqA or Dam that are required for sequestration after replication initiation are deleted, synchrony is lost and replication is initiated throughout the entire cell cycle [26,28]. Blocking of recently initiated origins during a so-called blocking period is therefore an essential mechanism to ensure synchronous replication initiation [Fig. 1(a)].

The combination of global oscillations in the initiation potential, which induce all origins to fire, and local origin sequestration, which prevents the newly replicated origins from reinitiation, appears to be an elegant solution to the problem of initiation synchrony. Yet, many questions remain. Newly replicated origins are only sequestered for a finite amount of time: the blocking period is about 10 min long [12,28,29]. Hence, while, after the initial origin has fired, the initiation potential must first continue to rise sufficiently long in order to allow all the remaining origins to fire, it must also come down before this blocking period is over because otherwise, the newly replicated origin(s) will fire again after all. The licensing period during which origins can fire must thus be long enough for all origins to fire, yet also shorter than the blocking period [Fig. 1(a)]. Given that the blocking period is only 10 min, this constraint is likely to pose a major challenge.

The problem of replication synchrony is compounded by the fact that the oscillations in the initiation potential are directly shaped by replication initiation itself [26]. When a new origin is fired, the newly generated replisomes will stimulate the deactivation mechanism called RIDA (regulatory inactivation of DnaA) [12,17,30,31]. Moreover, a few minutes after an origin has initiated DNA replication, the locus *datA* is duplicated, which enhances deactivation by stimulating the hydrolysis of ATP bound to DnaA [15,32–35]. Furthermore, the newly duplicated DNA will harbor new titration sites [13,22], which also tend to reduce the initiation potential by lowering the concentration of cytoplasmic DnaA. How these molecular mechanisms cause the initiation potential to first continue to rise during the licensing period and then fall before the blocking period is over is far from understood.

To study how replication can be initiated synchronously at several origins, we first propose a minimal coarse-grained model in which an initiation potential rises when the cell reaches a critical volume per origin. Each origin can initiate stochastically with a firing probability that depends on the initiation potential. The model contains a licensing period during which the initiation potential rises and origins can fire, and a blocking period during which newly fired origins cannot fire again. By varying the duration of the licensing and the blocking period we reveal four regimes. Only one of these gives rise to robust synchronous replication initiation. In particular, in order to initiate synchronously, the licensing period must be long enough for all origins to fire, yet shorter than the blocking period. However, given that the measured blocking period is only 10 min [12,28,29], the licensing period must be shorter than 10 min. To fire all origins within this short blocking period with a success rate of 92%, the firing rate must rise with the volume with a Hill coefficient of at least 20, such that the average time between the first and last initiation event is less than 4 min, as measured experimentally by Skarstad *et al.* [9]. Our modeling thus provides a rationale for the question of why DNA replication initiation in *E. coli* is so tightly controlled.

We then investigate how these general synchronization requirements could be realized in the bacterium *E. coli*, by replacing the coarse-grained initiation potential with our previously proposed molecular model, in which the free ATP-DnaA concentration oscillates over the course of the cell cycle [25]; to this end, we have extended this model to include stochastic origin firing. We find that if replication initiation is controlled by the DnaA activation switch [13,17,23,24], initiation synchrony is only achieved for a narrow range of parameters, which is hard to reconcile with the experimentally measured values. Adding titration [11,21,22] and bringing the system into a regime where the DnaA concentration in the cytoplasm is low during most of the cell cycle significantly improves the degree of synchrony by sharpening the rise of the initiation potential at a critical volume per origin. This suggests that combining a concentration cycle based on titration with a protein activation cycle is crucial for initiating replication synchronously at multiple origins in the bacterium *E. coli*.

II. THE LICENSING PERIOD MUST BE NONZERO AND SHORTER THAN THE BLOCKING PERIOD

To investigate the effect of stochastic replication initiation on the cell cycle of *E. coli*, we model the volume $V(t)$ of the cell as an exponential function, $V(t) = V_b\, e^{\lambda t}$, where the growth rate $\lambda = \ln(2)/\tau_d$, with cell-doubling time τ_d, is a model parameter. We track the number of chromosomes together with their state of replication (e.g., fully replicated or replication ongoing) and whenever an origin fires a new round of replication at time t^*, a new division time a constant cycling time τ_{cc} after replication initiation is set at $\tau_{div} = t^* + \tau_{cc}$. The constant cycling time τ_{cc} is given by the sum of the time to replicate the entire chromosome, T_C, and the time from the end of replication until cell division, T_D [Fig. 1(a)]. When the next division time is reached, the cell volume is divided by 2, and one of the two daughter chromosomes is kept at random for the next cell cycle. While our model follows the work of Cooper, Helmstetter, and Donachie [8,36] who proposed a tight coupling between cell division and replication initiation, a more loose coupling between replication and cell division has been suggested more recently [37,38]. Previous work has, however, shown that the replication initiation statistics are similar in models in which replication initiation is coupled more loosely to cell division because cell division does not significantly affect the replication-initiation cycle [25]. Importantly, the Cooper-Helmstetter-Donachie model is convenient because it ensures that cell division only happens when replication initiation has finished (see Appendix A for modeling details).

Our coarse-grained model to study the effect of stochastic replication initiation on the cell cycle consists of two parts. First, we model the available amount of initiator proteins in the cell as an initiation potential y that depends on the volume per origin, $v(t) = V(t)/n_{ori}(t)$, according to

$$y(v) = \frac{v^n}{v^n + v^{*n}} \tag{1}$$

with the Hill coefficient n and the critical volume per origin v^* [Fig. 1(b)]. Second, each origin is modeled as a two-state

system that can switch stochastically between an open and a closed configuration (see Appendix B for details). Exploiting that the origin is more likely to be in the open state when the initiation potential y in the cell is high, we assume that the probability to be in the open state p_o increases with the activation potential y as

$$p_o(y) = \frac{y^m}{y^m + y^{*m}} \tag{2}$$

with the Hill coefficient m and the critical initiation potential y^* [Fig. 1(c)]. Molecularly, this nonlinear opening probability $p_o(y)$ could arise via cooperative binding of the initiator to the origin, since the origin contains 12 DnaA binding sites [13]. Alternatively, it could arise via a Monod-Wyman-Changeux (MWC) model, where the open configuration becomes more energetically favorable the more initiators bind to the origin. Assuming rapid opening and closing dynamics of the origin, the origin firing rate is given by the probability to be in the open state, p_o, times the maximal firing rate k_f^0:

$$k_f = k_f^0\, p_o. \tag{3}$$

The model includes a licensing and blocking period, which are essential for synchronous replication initiation. In particular, at the critical volume per origin, v^*, the activation potential $y(t)$ rises, and the probability to initiate replication, $p_o(t)$, increases strongly [Eqs. (1) and (2); Fig. 1(d), second and third panels]. To study the effect of stochastic replication initiation on the degree of synchrony, we consider the fast growth regime ($\tau_d < \tau_{cc}$), where there are typically two or more origins in the cell at the moment of replication initiation. When the first origin fires, the number of origins in the cell increases stepwise, and the volume per origin, $v(t)$, drops instantaneously [Fig. 1(d)]. If the initiation potential $y(t)$ followed the change in the volume per origin instantaneously, it would become very unlikely for the second origin to initiate replication as well, resulting in asynchronous replication initiation. We therefore introduce a licensing time τ_l, during which the initiation potential does not yet sense the change in the volume per origin, $v(t)$, and continues to rise [Fig. 1(d), gray shaded area]. The opening probability $p_o(t)$ therefore rises sharply during this licensing time and the second origin also initiates replication stochastically. To prevent that already initiated origins fire again, we additionally introduce a blocking period τ_b, during which replication cannot be initiated again at the same origin [Fig. 1(d), light blue shaded area]. At the end of the licensing time τ_l, the activation potential is updated according to the current number of origins in the cell, and it thus drops instantaneously [Fig. 1(d), fourth panel].

To quantify the degree of synchrony of replication initiation for a given parameter set, we define the degree of synchrony s as the change of the number of origins, Δn_{ori}, from the beginning of the initiation period t_i to the end of the initiation period t_f, relative to the number of origins, $n_{ori}(t_i)$, at the beginning of the initiation period [Fig. 2(a)]:

$$s = \frac{\Delta n_{ori}}{n_{ori}(t_i)} = \frac{n_{ori}(t_f) - n_{ori}(t_i)}{n_{ori}(t_i)}. \tag{4}$$

The beginning of the initiation period t_i is given by the time at which the first origin fires and the initiation period ends at $t_f = t_i + \tau_l$, when the licensing period of the first origin that has fired is over. When the degree of synchrony s is one, replication is initiated synchronously, as all origins that were present at the beginning of the initiation period have fired [Fig. 2(a)]. For $s < 1$ or $s > 1$, replication is under- or overinitiated, respectively [Fig. 2(a)].

By varying the duration of the licensing and the blocking period, we find four different synchronization regimes (Fig. 2). Yet, only in regime 4 is replication initiated synchronously [Fig. 2(b)]. In regime 1, the blocking period τ_b is too short and replication is severely overinitiated, such that no stable cell cycles can be obtained [Fig. 2(b), gray fields]. In regime 2, the licensing time τ_l is too short and we obtain a highly undersynchronized cell cycle: after each initiation event, the initiation potential drops rapidly, preventing further initiation events. In regime 3, the licensing and blocking times are long enough, but the licensing time is longer than the blocking period, $\tau_l > \tau_b$. As a result, origins that have already fired can fire again after the end of the licensing period. In this third regime, the number of origins goes from one to four during one initiation duration instead of oscillating between two and four. We therefore call this regime "oversynchronized." Only in regime 4, where the licensing period τ_l is sufficiently large and the blocking period is even larger, $\tau_b > \tau_l$, is replication initiated synchronously [Fig. 2(b), regime 4].

III. A STEEP RISE IN THE ORIGIN OPENING PROBABILITY IS ESSENTIAL

Figure 2 clearly shows that the licensing period has to be smaller than the blocking period, but how small can it be? How does the degree of synchrony vary with τ_l? To answer this question, we compute the probability that two consecutive firing events happen within a time interval Δt smaller than the licensing time τ_l. To this end, we first derive an expression for the instantaneous firing probability $k_f(t) = k_f^0\, p_o(t)$. In our model, the opening probability $p_o(y)$ depends indirectly on the time-dependent volume per origin, $v(t)$, via the activation potential $y(v)$ [see Eqs. (1) and (2)]. The opening probability as a function of the volume per origin, v, can, however, be approximated by a Hill function (see Appendix C for derivation)

$$p_o(v) \approx \frac{v^{n_{eff}}}{v^{n_{eff}} + v^{*n_{eff}}} \tag{5}$$

with the effective Hill coefficient

$$n_{eff} = \frac{n\,m}{2}. \tag{6}$$

This is a good approximation for the opening probability $p_o(y(v))$, when both the Hill coefficient of the activation potential and that of the opening probability, n and m, respectively, are relatively high [see Eqs. (1) and (2) and Figs. 6(c) and 6(d)]. The firing rate is then given by Eq. (3) with the approximate opening probability $p_o(v)$ from Eq. (5). Using this approximation for the opening probability in the regime of sufficiently high Hill coefficients n and m, we can now calculate the probability that two independent initiation events at times t_1 and $t_2 > t_1$ happen within a time interval $\Delta t = t_2 - t_1 \leqslant \tau_l$ (Appendixes D and E). In order to compare this probability $\langle P(\Delta t < \tau_l)\rangle$ to the degree of synchrony obtained from the simulations in the growth regime where two origins are present at the beginning of an initiation event, we rescale

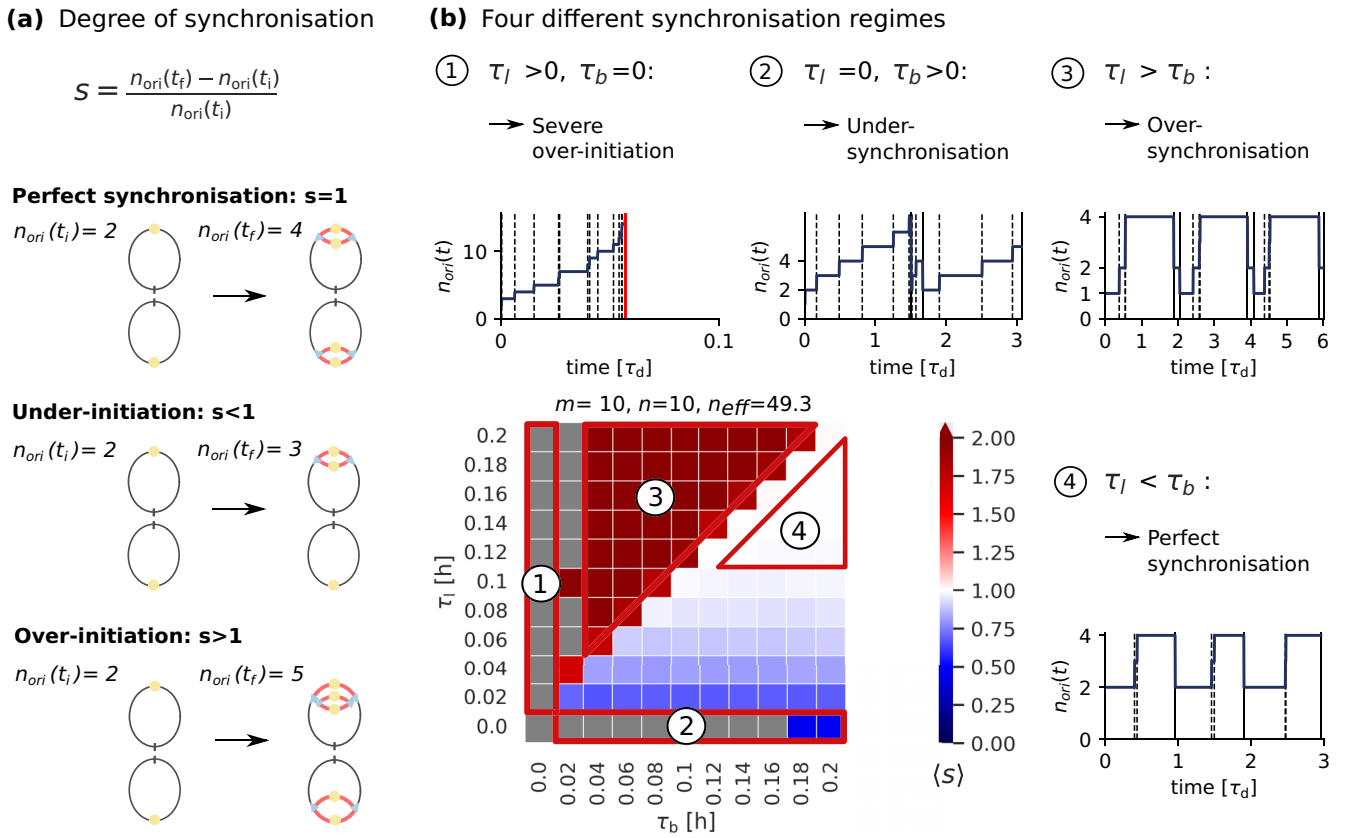

FIG. 2. Replication is only initiated synchronously when the licensing period is sufficiently long, yet shorter than the blocking period. (a) The degree of synchrony s of an initiation cascade is given by the number of origins at the end of the initiation cascade, $n_{\mathrm{ori}}(t_{\mathrm{f}})$, minus the number of origins at the beginning of the initiation cascade, $n_{\mathrm{ori}}(t_{\mathrm{i}})$, relative to the number of origins at the beginning of the initiation cascade, $n_{\mathrm{ori}}(t_{\mathrm{i}})$. An initiation cascade begins with the moment where the first origin fires and ends after the licensing time τ_{l}. Replication is initiated synchronously when all origins that were present at the beginning of the cascade have fired exactly once during the cascade ($s = 1$) and replication was under- or overinitiated when less or more origins have initiated, respectively. (b) The average degree of synchrony $\langle s \rangle$ as a function of the licensing period τ_{l} and the blocking period τ_{b}. The effective Hill coefficient n_{eff} is obtained by fitting the opening probability $p_{\mathrm{o}}(f(v))$ to a Hill function $p_{\mathrm{o}}(v)$ (Appendix C). For each parameter set, the average degree of synchrony was obtained from $N = 5000$ consecutive cell cycles. We show example time traces of the number of origins as a function of time (in units of the doubling time of the cell, τ_{d}) for four different synchronization regimes as indicated in the heatmap. When no cell cycle could be obtained, the field in the heatmap is marked in gray. (See Table I for all parameters.)

the probability to range from $s_{\min} = 0.5$ to $s_{\max} = 1$:

$$s_{\mathrm{th}} = 0.5 + \langle P(\Delta t < \tau_{\mathrm{l}}) \rangle \times 0.5. \tag{7}$$

This fairly simple model describes the average degree of synchrony $\langle s \rangle$ as a function of the licensing period τ_{l} for different Hill coefficients n and m remarkably well [Fig. 3(a)]. The transition from the undersynchronized to perfect synchronization regime in Fig. 2(b) is therefore given by the probability that two independent origin firing events happen within a short time window given by the licensing time τ_{l}. The higher the effective Hill coefficient n_{eff}, the higher the degree of synchrony for a given delay period τ_{l} [Fig. 3(a)]. The degree of synchrony $\langle s \rangle$ increases with the effective Hill coefficient because that raises the firing rate more steeply, making it more likely that the two origins fire within the licensing time τ_{l}.

While the degree of synchrony $\langle s \rangle$ increases with the licensing time τ_{l}, τ_{l} cannot be longer than the blocking period τ_{b}, because otherwise origins that have already fired will fire again. The blocking period thus bounds τ_{l}. The duration of the blocking period, as set by the binding of SeqA to the origins, is about 10 min [12,28,29]. As the licensing time must be shorter than the blocking period to prevent overinitiation [Fig. 2(b), regime 3], the licensing time in *E. coli* must thus be less than $\tau_{\mathrm{b}}^{\mathrm{expt}} = 10$ min. Figure 3(a) shows that this puts a major constraint on the Hill coefficient: to get a degree of synchrony $\langle s \rangle$ that is above 95%, the effective Hill coefficient must be at least $n_{\mathrm{eff}} = 30$.

The question remains what the effective Hill coefficient n_{eff} is that is consistent with experiments. Interestingly, Skarstad *et al.* measured the time between the first and last firing event, which we can compare against our theoretical prediction [9]. However, to do so, we must first examine the dependence on the growth rate, because Skarstad *et al.* performed their measurements at a higher growth rate. Figure 7 shows that while the average degree of synchrony $\langle s \rangle$ as a function of the licensing time τ_{l} varies strongly with the effective Hill coefficient n_{eff}, it is fairly independent of the doubling time of the cell, τ_{d}.

Given that $\langle s \rangle$ as a function of τ_{l} is fairly independent of the growth rate, we now examine the data of Skarstad

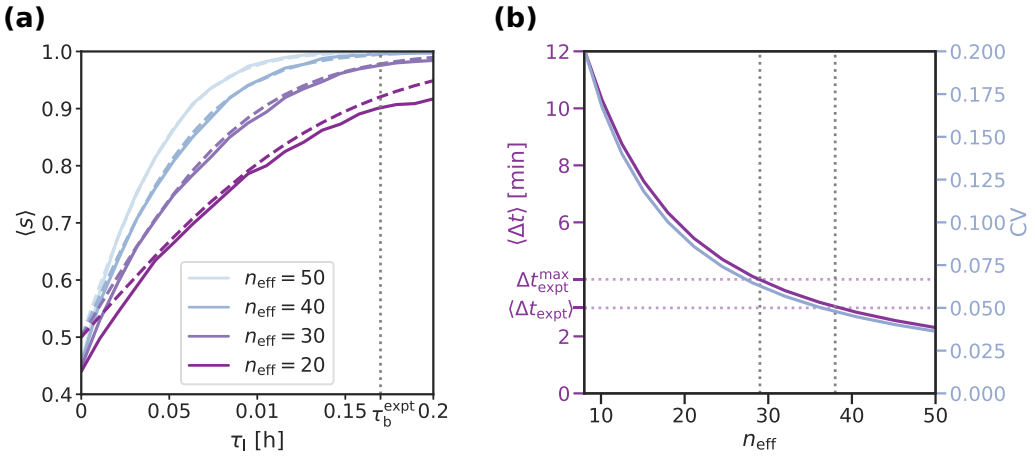

FIG. 3. The experimentally observed high precision of replication initiation is required to ensure synchronous replication initiation at multiple origins. (a) The average degree of synchrony $\langle s\rangle$ as a function of the licensing time τ_l for varying effective Hill coefficients $n_{\rm eff}$ (with $n = m = \sqrt{2\,n_{\rm eff}}$) from the simulations (solid lines) agrees well with the theoretical prediction derived in Appendix E (dashed lines). The small difference between the simulations and theory at very low delay periods arises from the fact that while in the theory for two synchronous firing events, the minimal degree of synchrony is $s_{\rm min} = 0.5$, in the simulations there can be more origins at the beginning of an initiation cascade, leading to a lower degree of synchrony $s_{\rm min} < 0.5$. In these simulations, the blocking period τ_b is set larger than all tested licensing τ_l periods ($\tau_b = 0.25$ h), such that overinitiation events cannot occur. The maximal firing rate k_f^0 is set such that the average initiation volume $\langle v^*\rangle$ equals the theoretical initiation volume v^* in Eq. (5) as explained in Appendix D. The experimentally measured blocking period $\tau_b^{\rm expt}$ is marked as a gray vertical dotted line. For each parameter set, the average degree of synchrony was obtained from $N = 5000$ consecutive cell cycles. (b) The theoretical average time interval between two consecutive firing events $\langle\Delta t\rangle$ (pink line and axes) and the coefficient of variation of the initiation volume (CV, blue line and axes) as a function of the effective Hill coefficient $n_{\rm eff}$ (see Appendix F for derivation). Skarstad *et al.* [9] found experimentally that the average time interval to fire all origins in the B/r A *E. coli* strain is about $\langle\Delta t_{\rm expt}\rangle = 3$ min with an upper estimate of $\Delta t_{\rm expt}^{\rm max} = 4$ min (horizontal dotted pink lines). The effective Hill coefficient lies therefore in the range $n_{\rm eff} = 29$–38 (vertical dotted gray lines), corresponding to a coefficient of variation of CV = 0.05–0.07. This agrees well with the experimentally measured precision of the initiation volume of CV $\leqslant 0.1$ [2,7,37]. Interestingly, the average degree of synchrony at $n_{\rm eff} = 30$ and $n_{\rm eff} = 40$, respectively, is given by $\langle s\rangle(n_{\rm eff} = 30) = 0.975$ and $\langle s\rangle(n_{\rm eff} = 40) = 0.996$, corresponding to the probabilities to fire all origins synchronously of $\langle P(\Delta t < \tau_l)\rangle(n_{\rm eff} = 30) \equiv P_s(n_{\rm eff} = 30) = 95.5\%$ and $P_s(n_{\rm eff} = 40) = 98.9\%$. This prediction of the degree of synchrony agrees well with the qualitative experimental observation that in *E. coli* DNA replication is typically initiated synchronously at multiple origins. Our model therefore provides a rationale for the experimentally observed high precision of replication initiation. (See Table I for all parameters.)

et al. [9]. To obtain an experimental estimate for the effective Hill coefficient and thus for the average degree of synchrony, we calculate the average time interval between the first and last initiation events $\langle\Delta t\rangle$ (see Appendix F) and compare it to the experiments. Skarstad *et al.* find that this time is on average $\langle\Delta t_{\rm expt}\rangle \approx 3$ min with an upper limit of $\Delta t_{\rm expt}^{\rm max} \approx 4$ min [9]. Our theory predicts that to fire two initiation events within an average time interval of $\langle\Delta t\rangle = 3$–$4$ min, the effective Hill coefficient must be in the range $n_{\rm eff} = 29$–38 [Fig. 3(b), vertical gray dotted lines]. Interestingly, the dependence of $\langle\Delta t\rangle$ on $n_{\rm eff}$ closely tracks that of the coefficient of variation (CV) of the initiation volume [Fig. 3(b)]. The $\langle\Delta t\rangle = 3$–$4$ min measured by Skarstad *et al.* corresponds to a CV of the initiation volume CV ≈ 0.05–0.06. This agrees fairly well with the experimental finding that the initiation volume is one of the most tightly controlled cell cycle parameters with CV = 0.08–0.1 [2,37]. A CV of 0.1 as measured by Ref. [2] corresponds to $n_{\rm eff} \approx 20$ [Fig. 3(b), see also calculation in Ref. [2]] and would thus only result in a relatively low degree of synchrony of less than $\langle s\rangle = 0.92$ corresponding to a probability of initiating synchronously of $\langle P(\Delta t < \tau_l)\rangle \equiv P_s = 84\%$ [see Eq. (7)]. Recent experiments show, however, that the contribution from the intrinsic noise in replication initiation to the CV is only about CV$_{\rm int} = 0.04$–0.05 [7], in even better agreement with the Skarstad data [Fig. 3(b)]. Our model, which only concerns the effect of intrinsic noise, then predicts that for this low CV$_{\rm int}$ the effective Hill coefficient $n_{\rm eff}$ must be at least 40 [Fig. 3(b)], which then means that at least $P_s = 98\%$ of the initiation events happen synchronously within a period of 10 minutes corresponding to $\langle s\rangle = 0.99$ [Fig. 3(a)].

Before we conclude, we must discuss one key parameter, which is the maximal firing rate k_f^0. In our theoretical model, we covaried k_f^0 with $n_{\rm eff}$ to keep the average initiation volume per origin, $\langle v^*\rangle$, constant and equal to v^* of Eq. (5), following the procedure of Wallden *et al.* [2] (see Appendix D). Figure 8(a) shows $\langle\Delta t\rangle$ in our theoretical model as a function of k_f^0 and $n_{\rm eff}$ separately (thus without enforcing the constraint $\langle v^*\rangle = v^*$). While $\langle\Delta t\rangle$ increases with both k_f^0 and $n_{\rm eff}$, there is a minimal $n_{\rm eff}$ that is necessary to reach a given $\langle\Delta t\rangle$, corresponding to the limit $k_f^0 \to \infty$ [see inset of Fig. 8(a)]. The Hill coefficient necessary to reach the $\langle\Delta t\rangle$ that matches the value measured by Skarstad *et al.* is lower than that in the above procedure in which k_f^0 and $n_{\rm eff}$ are covaried [corresponding to the diagonal in Fig. 8(a)], but it is still very high, around $n_{\rm eff} \approx 20$ [Fig. 8(a)]. Figure 8(b) shows that in

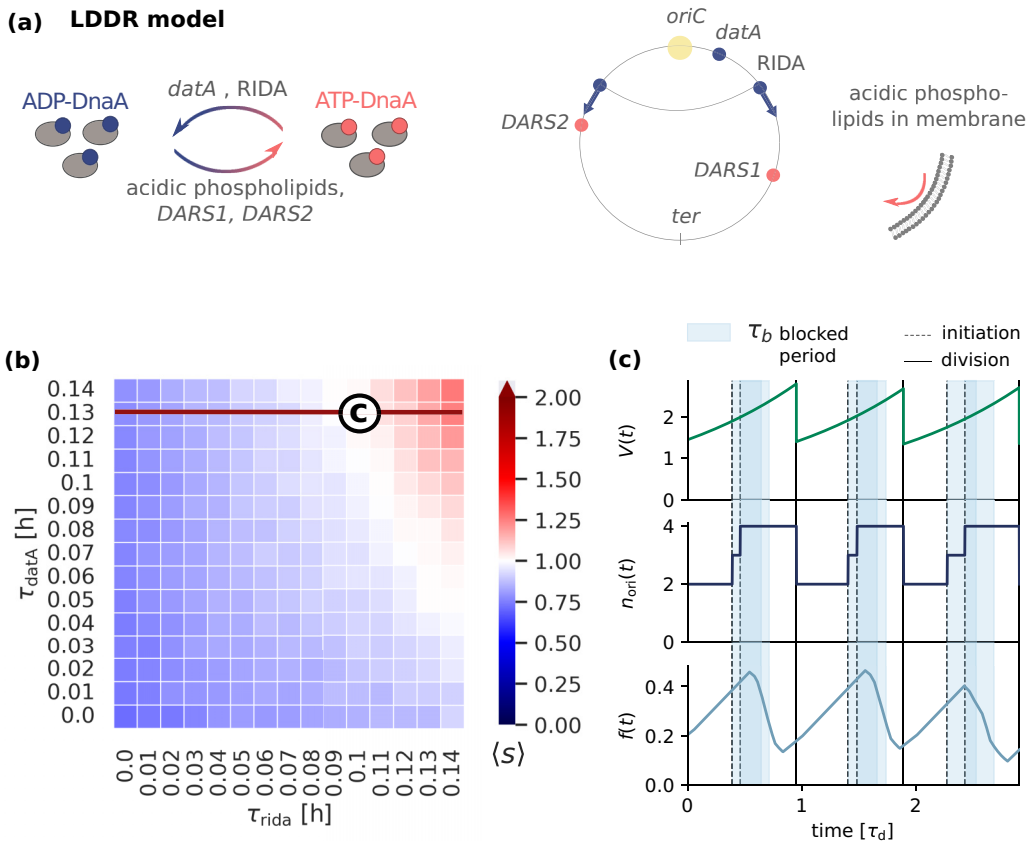

FIG. 4. The LDDR model can ensure a high degree of synchronous replication initiation for a narrow range of parameters. (a) In the lipid-*datA*-*DARS1*/*2*-RIDA (LDDR) model, replication forks overlap and RIDA is the main deactivator in combination with the activators *DARS1* and *DARS2*. (b) The average degree of synchrony, $\langle s \rangle$, as a function of the replication time of the site *datA*, τ_{datA}, and the onset time of RIDA, τ_{rida}. The sites *DARS1* and *DARS2* are replicated at the experimentally measured times $\tau_{\mathrm{d1}} = 0.25\,\mathrm{h} = 15\,\mathrm{min}$ and $\tau_{\mathrm{d1}} = 0.4\,\mathrm{h} = 24\,\mathrm{min}$, respectively. Replication is only initiated synchronously for a small range of parameters: when the site *datA* is replicated after the experimentally measured time of $\tau_{\mathrm{datA}} = 0.13\,\mathrm{h} \approx 8\,\mathrm{min}$ (red horizontal line), replication in the LDDR model is only initiated synchronously if RIDA starts only about 6 min after the origin is initiated. It is, however, not clear what could cause a delay of 6 min in the onset of RIDA. (c) The volume $V(t)$, the number of origins, $n_{\mathrm{ori}}(t)$, and the ATP-DnaA fraction $f(t)$ as a function of time (in units of the doubling time of the cell, τ_{d}) for the parameter combination marked in (b). The large amplitude oscillations in the active fraction in combination with a long delay in the onset of deactivation via RIDA and *datA* can give rise to a high degree of synchrony for a small range of parameters. For each parameter set in (b), the average degree of synchrony was obtained from $N = 5000$ consecutive cell cycles. (See Table I for all parameters.)

this limit, $k_{\mathrm{f}}^{0} \to \infty$ and $n_{\mathrm{eff}} = 20$, the degree of synchrony is very high, with $P_{\mathrm{s}} = 92\%$. Our model of stochastic replication initiation thus provides a rationale for the experimentally observed high precision of DNA replication initiation in *E. coli*: given the constraint set by the duration of the blocking period, the system requires a very high Hill coefficient in order to initiate replication synchronously. Since increasing the Hill coefficient beyond this already large value becomes progressively harder, it seems that the system operates close to what is theoretically possible given the duration of the blocking period.

IV. INITIATION SYNCHRONY IN MOLECULAR ACTIVATION SWITCH MODEL FOR *E. coli*

Our coarse-grained model of replication initiation revealed general requirements for initiating replication synchronously at several origins. It remains, however, an open question how these requirements are implemented on a molecular level in different organisms. In *E. coli*, both a protein activation cycle and a concentration cycle are required for robust replication initiation at all growth rates [25]. In the following, we first address the question whether a protein activation cycle alone, i.e., without the help of a concentration cycle, can yield synchronous replication. To this end, we will study the so-called lipid-*datA*-*DARS1*/*2*-RIDA (LDDR) model, which we developed previously [25] [Fig. 4(a)]. This model contains activation of DnaA via the lipids and the chromosomal sites DARS1/2 and deactivation of DnaA via the chromosomal site *datA* and the replication-associated mechanism of regulatory inactivation of DnaA (RIDA) [25]. We show that this cycle alone can induce synchronous replication initiation, but only over a very limited parameter regime. In a second step, we show that adding a concentration cycle via titration sites can significantly enhance the degree of synchrony. To test the effect of stochastic origin firing in the LDDR model, we replace the abstract initiation potential $y(v)$ we used in the

coarse-grained model with the LDDR model for the ATP-DnaA fraction $f(t)$ in the cell. The opening probability $p_o(f)$ is again modeled as a simple Hill function according to Eq. (2). Motivated by the experimental observation that there are about ten sites for DnaA binding to the origin [13], the Hill coefficient was chosen to be $m = 10$; in addition, the critical fraction in Eq. (2) was chosen to be $f^* = 0.5$. Moreover, the maximal firing rate k_f^0 was set to a large value, i.e., $k_f^0 = 1000\ \mathrm{h}^{-1}$, such that the system is in the regime where the degree of synchrony is not limited by k_f^0 [see Fig. 8(b)], but only limited by the dynamics of the activation cycle $f(t)$. Like in the coarse-grained model, already initiated origins are blocked transiently during a blocking period of $\tau_b = 10$ min. Contrary to the coarse-grained model, where after the end of the licensing period the initiation potential drops instantaneously to a very low value, in the LDDR model, the active fraction f follows from the temporal dynamics of the antagonistic interplay between DnaA activation and deactivation (see Appendix G for details). In the LDDR model, the licensing period is thus not imposed, as in the coarse-grained model above, but is implicit in the dynamics of the LDDR model. Yet, to quantify the degree of synchrony, we need to define an effective initiation period τ_i, akin to the licensing period τ_l in the coarse-grained model [see Eqs. (4) and (7)]. We define τ_i to be a fraction of the cell cycle time τ_d: $\tau_i = \alpha\, \tau_d$. While α cannot be defined uniquely, we show in Appendix H that the degree of synchrony is fairly robust to the precise choice of α. In the following, we therefore choose $\alpha = 0.4$, such that $\tau_i = 0.4\, \tau_d$.

The LDDR model can indeed give rise to synchronous replication initiation at multiple origins, but only for a small range of parameters: when the (de)activators *DARS1*, *DARS2*, and *datA* are located at the experimentally measured positions on the chromosome, replication is initiated asynchronously when RIDA starts directly after an origin has fired [Fig. 4(b) at $\tau_{rida} = 0$ h]. As RIDA is a strong deactivator, it causes the active fraction to drop rapidly after the first origin has been initiated and thus prevents other origins from firing as well. By varying both the position of *datA* on the chromosome and the time at which RIDA starts after an origin has fired, we find that replication can be initiated synchronously in the LDDR model for a small range of parameters: at the experimentally measured replication time of *datA* of $\tau_{datA} = 0.13\,\mathrm{h} \approx 8\,\mathrm{min}$ [13,32], replication is initiated with a high degree of synchrony when the deactivation rate of RIDA becomes high with a delay of $\tau_{rida} = 0.1\,\mathrm{h} = 6$ min after the origin has fired [Figs. 4(b) and 4(c)]. The closer the site *datA* is to the origin, the later RIDA should start for synchronous replication initiation [Fig. 4(b)].

It remains, however, unclear what molecular mechanism could cause a delay in the onset of RIDA of about 6 min. In RIDA, the DNA polymerase clamp on newly synthesized DNA forms a complex with ADP and the Hda protein. The resultant ADP-Hda-clamp-DNA can bind ATP-DnaA and stimulates ATP hydrolysis yielding ADP-DnaA [30,31]. It is conceivable that Hda binding is slow, but whether it would yield a delay of about 6 min is far from clear. For experimentally realistic parameters, the LDDR model appears therefore insufficient to explain synchronous replication initiation in *E. coli*.

V. TITRATION CAN ENHANCE THE DEGREE OF SYNCHRONY OF AN ACTIVATION SWITCH

In *E. coli*, DNA replication initiation is not only controlled via an activation switch but also via titration [10,11]. To study the effect of titration on the degree of synchrony, we add homogeneously distributed titration sites on the chromosome to the LDDR model [25]. In the LDDR-titration model, the initiation potential is given by the free ATP-DnaA concentration $[D]_{ATP,f}$ in the cell and both oscillations in the active fraction f and in the free DnaA concentration $[D]_{T,f}$ contribute to regulating replication initiation (see Appendix I for details). We again model the stochastic opening probability of the origin as a Hill function [Eq. (2)] with Hill coefficient $m = 10$. The critical initiation potential y^* is now given by a critical free ATP-DnaA concentration $[D]^*_{ATP,f}$ at which ATP-DnaA binds cooperatively to the origin. We here neglect the effect of the relatively small number of about 10–20 DnaA proteins that are bound to the origin on the free DnaA concentration. As explained in Ref. [25], we set the parameters (by varying the lipid activation rate α_l) such that the initiation volume of the switch, v_s^*, and the initiation volume of the titration mechanism, v_t^*, are approximately the same. This optimal choice ensures that both the free concentration and the active fraction rise at the same critical volume per origin, thus increasing the amplitude of the oscillations in the free ATP-DnaA concentration.

Figures 5(a) and 5(c) show the time traces of the model that combines titration with the activation switch. The small jump in the total free DnaA concentration upon cell division results from the following interplay. First, only one out of two chromosomes is selected per daughter cell [Figs. 5(a) and 5(c), second panel). The stochastic firing of the origins causes a temporal delay between the initiation of replication at the respective origins. Moreover, in the growth-rate regime of overlapping replication forks considered here, not all chromosomes have been fully replicated at the moment of cell division. Taken together, this means that at the moment of cell division not all chromosomes have the same number of titration sites (the sites are distributed uniformly). The difference in the number of titration sites per chromosome causes a slight change in the free concentration upon cell division.

Adding titration sites to the LDDR model affects the degree of synchrony only little when the critical free ATP-DnaA concentration at which replication is initiated is high. When a new round of replication is initiated, new titration sites are generated and the free DnaA concentration drops. As discussed in Ref. [25], at high growth rates, where multiple chromosomes are present in the cell, new titration sites are, however, replicated at a similar rate as new DnaA proteins are synthesized. Titration therefore introduces only weak oscillations in the free total DnaA concentration [Fig. 5(a)]. If the critical free DnaA concentration at which DNA replication is initiated is relatively high, the oscillations in the free DnaA concentration contribute only little to the oscillations in the initiation potential [Fig. 5(a)]. In this scenario, adding titration to the LDDR model does not significantly change the degree of synchrony, the optimal position of *datA* on the chromosome, or the optimal onset time of RIDA [compare Fig. 5(b) to Fig. 4(b)].

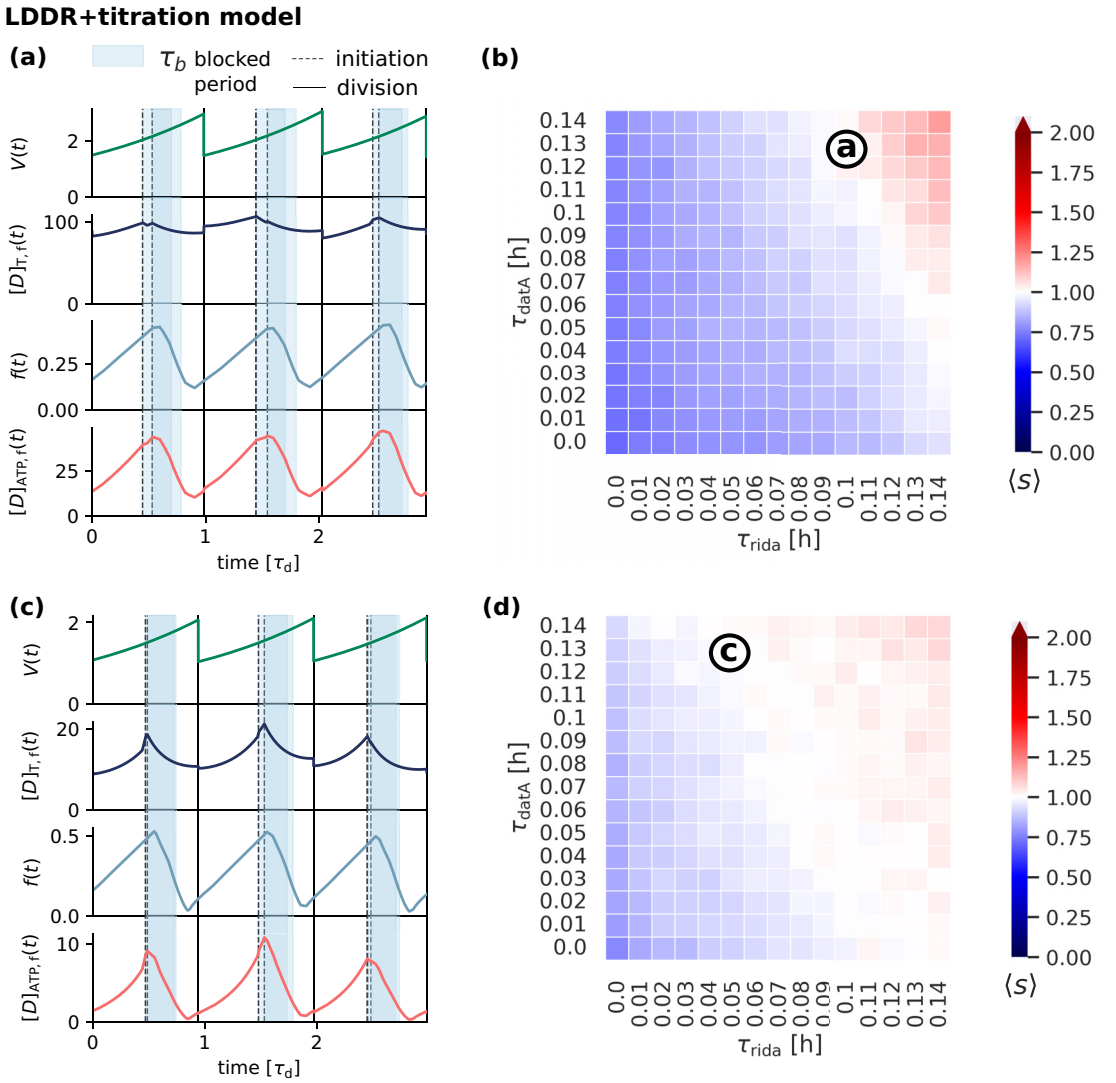

FIG. 5. Adding titration sites to the LDDR model enhances initiation synchrony for low critical free DnaA concentrations. [(a), (c)] The volume $V(t)$, free DnaA concentration (independent of whether DnaA is bound to ATP or ADP) $[D]_{T,f}(t)$, the ATP-DnaA fraction $f(t)$, and the free ATP-DnaA concentration $[D]_{ATP,f}(t)$ as a function of time (in units of the doubling time of the cell, $\tau_d = 0.67\,\text{h} = 40\,\text{min}$) for a critical free ATP-DnaA concentration of (a) $[D]^*_{f,ATP} = 50\,\mu\text{m}^{-3}$ and (c) $[D]^*_{f,ATP} = 10\,\mu\text{m}^{-3}$. During the blocking period τ_b (light blue shaded area), the newly replicated origins cannot be reinitiated. (a) When the critical free ATP-DnaA concentration is relatively high, the free DnaA concentration $[D]_{T,f}(t)$ oscillates only weakly and decreases slightly after new rounds of replication are initiated due to the synthesis of new sites. The shape of the oscillations in the free ATP-DnaA concentration $[D]_{ATP,f}(t)$ is therefore mainly determined by the oscillations in the ATP-DnaA fraction $f(t)$. [(b), (d)] The average degree of synchrony $\langle s\rangle$ as a function of the replication time of the site *datA*, τ_{datA}, and the onset time of RIDA, τ_{rida}, for (b) $[D]^*_{f,ATP} = 50\,\mu\text{m}^{-3}$ and (d) $[D]^*_{f,ATP} = 10\,\mu\text{m}^{-3}$. The sites *DARS1* and *DARS2* are replicated at the experimentally measured times $\tau_{d1} = 0.25\,\text{h} = 15\,\text{min}$ and $\tau_{d1} = 0.4\,\text{h} = 24\,\text{min}$, respectively. (b) When the critical free ATP-DnaA concentration is high, the effect of the titration sites on the degree of synchrony is small and almost indistinguishable from the scenario without titration sites [compare to Fig. 4(b)]. (c) At a lower critical free ATP-DnaA concentration, the oscillations in the free concentration are larger and lead to sharper oscillations of the free ATP-DnaA concentration. This causes a broader range of parameters for which replication is initiated synchronously (d). For each parameter pair in (b) and (d), the average degree of synchrony was obtained from $N = 5000$ consecutive cell cycles. (See Table I for all parameters.)

When the free DnaA concentration $[D]_{T,f}$ is low, however, titration can significantly enhance the degree of synchrony of the LDDR model. Setting the critical free ATP-DnaA $[D]^*_{f,ATP}$ to a value that is comparable to the affinity of the titration sites increases the oscillations in the free DnaA concentration [Fig. 5(c)]. The resulting sharper rise of the free ATP-DnaA concentration gives rise to a higher degree of synchrony at all positions of *datA* and onset times of RIDA [Fig. 5(c)]. The regime of parameters in which replication is initiated with a high degree of synchrony now extends also to shorter and more realistic onset times of RIDA than in the LDDR model [Fig. 5(d)]. In summary, the full titration-switch model is able to synchronously initiate replication.

VI. DISCUSSION

The bacterium *E. coli* initiates replication at several origins synchronously with high precision. How it achieves this high degree of synchrony remained, however, unknown. In this work, we have revealed several general principles that govern whether replication is initiated synchronously at several origins: (1) the initiation potential must remain high after the first origin has fired so that the remaining origins can fire; (2) origins that have already fired must be prevented from reinitiating immediately as long as not all origins have fired; this necessitates a blocking period and (3) the initiation potential must come down before the blocking period is over to prevent reinitiation of the newly replicated origins. The licensing period, during which the origins can fire, must thus be shorter than the blocking period. The blocking period, in turn, is limited to only 10 min [12,28,29], which means that the licensing period must be shorter than 10 min. To ensure that all origins fire during this short licensing period, the initiation potential must rise sharply, and to guarantee that the initiation potential is low again before the blocking period is over, it also must fall sharply. Synchronous replication initiation thus requires sharp oscillations in the initiation potential. Such oscillations will also give rise to small variations in the initiation volume. Our modeling thus reveals that the experimentally observed small variation in the initiation volume is a result of the requirement of synchronous replication initiation.

Our minimal, coarse-grained model has been instrumental in elucidating the principal requirements for synchronous replication initiation. This model is inspired by our molecular model of Ref. [25], which, in turn, is based on experimental data. The main assumption is that the dynamics of the initiation potential, the free concentration of active DnaA, is in quasiequilibrium with respect to the volume dynamics. This assumption is reasonable because DNA binding and DnaA (de)activation rates are an order of magnitude faster than the (highest) growth rate [25]. Given this quasiequilibrium assumption, the model then exploits that a Hill function is an accurate, effective description of ultrasensitive systems, irrespective of the underlying molecular mechanisms. The other assumption is that the only source of stochasticity is in the opening of the origin; we have neglected the stochasticity in the initiation potential. This serves to put a bound on the precision of initiation (a lower bound on the CV of the initiation volume and an upper bound on the degree of synchrony) and hence a lower bound on the minimally required effective Hill coefficient. Indeed, including noise in the initiation potential would raise the minimally required Hill coefficient only further.

The minimal model shows that the effective Hill coefficient must be at least 20, raising the question what are the molecular mechanisms that give rise to such a high Hill coefficient. First, our minimal model shows that the sharp dependence of the opening probability on the initiation potential and the steep dependence of the latter on the volume multiply to give an even higher Hill coefficient [see Eq. (6)]. In addition, each of the two processes separately is likely to have a high Hill coefficient. The origin has 12 binding sites for DnaA [13], thus allowing for a strong cooperative, nonlinear response of the opening probability to the rise in the DnaA concentration; an opening mechanism based on an MWC would allow for an even stronger response. Concerning the dependence of the initiation potential on the cell volume, our previously developed model [25] predicts that there are two mechanisms that act in concert to give rise to a steep dependence. The first mechanism is associated with the concentration cycle of DnaA based on titration. After a new round of replication has been initiated, the newly synthesized DnaA proteins strongly bind to sites on the DNA that are uniformly distributed over the chromosome, such that the free cytoplasmic concentration initially remains low; yet, after all titration sites have been occupied, the free concentration rises sharply, inducing an ultrasensitive response [39]. The second mechanism is associated with the activation cycle of DnaA. DnaA switches between an active and an inactive form via a push-pull mechanism based on the antagonistic interplay between DnaA activation (via synthesis, lipids, and *DARS1/2*) and DnaA deactivation (via RIDA and *datA*) [25]. This antagonism gives rise to a "zero-order" ultrasensitive response when the (de)activation mechanisms operate near saturation and hence become nearly independent of the substrate (DnaA) concentration [40]. Since the number of DnaA proteins is much larger than the number of *datA*, *DARS1/2*, and binding sites on the replication fork (enabling RIDA), it is quite likely that also in this system the (de)activation mechanisms operate near saturation, and thereby generate a zero-order ultrasensitive response. Last, the interplay between the concentration cycle, which generates oscillations in the *free concentration* of DnaA, and the activation cycle, which generates oscillations in the *active fraction* of DnaA, gives rise to even sharper oscillations in the *active free concentration* [25].

That the combination of a concentration and an activation cycle can indeed generate oscillations in the initiation potential that are sharp enough for synchronous replication initiation is supported by the simulations of our previously presented model *E. coli* [25]. It can ensure a high degree of initiation synchrony for a range of parameters that agree with the experimentally measured ones. We find that if replication initiation is governed by a protein activation switch only, the optimal onset time of the RIDA mechanism would have to be about 6 min in order to ensure synchronous replication initiation. As RIDA is coupled to active replication [41], protein diffusion in cells is typically on the order of seconds rather than minutes [42] and binding of Hda to the replication clamps is rather strong [30,31], it seems natural to assume that the deactivation via RIDA becomes strong directly after a new round of replication starts. It is, however, conceivable that Hda concentration rises slowly, that Hda binding is slow, or that several RIDA complexes are required for a strong deactivation rate of RIDA [30,31]. Adding a concentration cycle based on titration sites to the activation switch and bringing the system to a regime where the free DnaA concentration is low during the entire cell cycle enhances the degree of synchrony significantly for a broad range of parameters. Importantly, in the combined model, replication is initiated with a high degree of synchrony also for shorter onset times of RIDA. Combining an activation cycle with a concentration cycle is therefore likely to be vital to synchronous replication initiation in *E. coli*.

To verify our model and make novel predictions, we turn to the key parameters of our coarse-grained model, which are (1) the duration of the blocking period τ_b, (2) the duration of the licensing period τ_l, and (3) the effective Hill coefficients with which the initiation potential and the firing probability rise during the cell cycle. The most important prediction of our model, namely, that the licensing period τ_l must be sufficiently long so that all origins fire within this time, yet shorter than the blocking period τ_b to prevent reinitiation, is strongly supported by experiments. As the blocking period is a direct consequence of origin sequestration via SeqA its duration τ_b can be varied, both in experiments and in our simulations. Our model predicts that while increasing the duration of the blocking period does not change the degree of synchrony (provided it remains shorter than the cell division time τ_d), decreasing the duration of the blocking period such that it becomes shorter than the licensing period τ_l, i.e., $\tau_b < \tau_l$, leads to strong overinitiation and asynchrony [see Fig. 2(b)]. Interestingly, experiments confirm these predictions: prolonging the blocking period of wild-type cells by introducing excess SeqA in the cell does not affect the degree of synchronization [26,43,44]. Shortening the blocking period by increasing the levels of Dam resulting in faster remethylation rates leads, however, to asynchronous initiation [26,45,46].

The latter two parameters of our model, namely, the licensing period and the effective Hill coefficient, are both characteristics of the temporal variations in the initiation potential. Therefore, these two parameters are intertwined and are difficult to manipulate separately. Experiments show that mutations in *datA*, *Hda*, *DASR2*, *ihf*, and *fis* that affect the (de)activators of DnaA lead to asynchronous replication initiation [26]. Interestingly, recent experiments show that also the CV of these mutant cells is increased [7]. While these mutations in (de)activators of DnaA likely affect both the duration of the licensing period and the steepness of the rise in the initiation potential, they nevertheless verify one of our predictions, namely, that the variance in the initiation volume and the degree of synchronization are correlated. Importantly, this is an outcome from our model that we did not put in *a priori*.

Besides these already verified predictions, we also make testable predictions and propose experiments that can be used to test these predictions. In our detailed molecular model, the onset time of RIDA and the temporal delay in replicating the chromosomal site *datA* set the licensing time. While the onset time of RIDA seems hard to control, the position of *datA* on the chromosome can be varied and the resulting degree of synchrony can be measured. Our model makes the strong prediction that replication is only initiated synchronously for an optimal position of *datA* on the chromosome [Fig. 5(d)]. When *datA* is too close to the origin, τ_l becomes too short, the initiation potential drops too rapidly, and replication is underinitiated. When *datA* is, however, too far away from the origin, such that $\tau_l > \tau_b$, the initiation potential drops too late, and after the end of the blocking period overinitiation events should occur. Experiments indeed show that translocating the site *datA* to the terminus causes asynchronous replication initiation at high growth rates [33], strongly supporting our model. To test our model further, in these mutant cells the blocking period could be prolonged experimentally by introducing excess SeqA, such that, as before, $\tau_b > \tau_l$. Our model then predicts that this should reduce the degree of overinitiation.

To determine the effective Hill coefficient of the opening probability experimentally, its two contributions, namely, the nonlinear rise in the initiation potential $y(v)$ as a function of the volume v and the nonlinear firing probability of the origin, $p(y)$, as a function of the initiation potential y, need to be studied separately. The Hill coefficient n of the initiation potential as a function of the volume can be obtained by measuring the free ATP-DnaA concentration in the cell as a function of the cell volume over the course of the cell cycle, although these experiments have proven challenging so far. By mutating the (de)activators, one could then test our prediction that the steepness of the oscillations in ATP-DnaA is correlated with the precision of initiation. Second, the Hill coefficient of the opening probability as a function of the initiation potential could be obtained by measuring the origin firing rate at different initiator concentrations (ATP-DnaA concentration, total DnaA concentration, and ATP-DnaA fraction) *in vitro*, similar to the experimental procedure of Hwang *et al.* [47]. Then, by introducing different mutations, one could design mutants with a less sharp rise in the opening probability that could be used to test our predictions on the degree of synchrony and the coefficient of variation as a function of the Hill coefficient [Figs. 3(a) and 3(b)].

Increasing the duration of the blocking period would be an easy way for the cell to increase the degree of synchrony. However, also at very fast growth rates, where the doubling time of *E. coli* is about 20 min, the blocking period must remain shorter than the doubling time in order to allow for a new round of replication to start in time. This imposes a natural bound for the duration of the blocking period. Since the duration of the blocking period imposes a hard constraint on synchronous replication initiation, it is tempting to speculate that the requirement of synchronous replication initiation limits the maximal growth rate of *E. coli*.

Also other organisms such as the bacteria *Bacillus subtilis* [3,4], *Mycobacterium smegmatis* [5], and *Vibrio cholerae* [6] initiate multiple chromosomes synchronously in certain growth conditions. These bacteria are evolutionarily divergent and have different molecular mechanisms to control the initiation of replication. Nevertheless, the general principles for synchronous replication initiation presented in this work should also remain valid for these organisms. For example, while the bacterium *B. subtilis* lacks the protein SeqA, it instead contains the protein Spo0A, which can inhibit replication initiation in the *B. subtilis* phage $\phi 29$ *in vivo* and has been shown to bind to specific sites on the origin *in vitro* [12]. These experiments suggest that Spo0A, similar to SeqA in *E. coli*, represses chromosomal replication by binding directly to the origin region of *B. subtilis*.

Finally, we have not modeled the binding of about 10–20 ATP-DnaA proteins to the origin explicitly. It has, however, been proposed in the so-called initiation cascade model that initiating replication at the first origin could cause other origins to fire as well by releasing the bound initiator proteins into the cytoplasm [48,49]. The resulting higher concentration of free DnaA proteins could lead to a redistribution of the free DnaA proteins to the remaining origins, making the next

replication initiation event more likely [48]. We tested this idea by introducing weak, cooperative origin binding sites to which only ATP-DnaA can bind into our model. When in this extended model the concentration of ATP-DnaA in the cytoplasm rises, the weak binding sites at the respective origins begin to fill up and then trigger the initiation of replication at a randomly selected origin (see Appendix J). After replication has been initiated, the binding sites at the origin that fired become unavailable for binding DnaA for the duration of the blocking period, causing a rise in the free DnaA concentration, as predicted by Ref. [48]. We find, however, that the ATP-DnaA binding to the origin has two opposing effects: on the one hand, the initiation potential indeed increases right after the first initiation event due to the released ATP-DnaA proteins, making the next initiation event more likely [see Figs. 9(a) and 9(b)]. On the other hand, binding of ATP-DnaA proteins to the origin leads to a less sharp rise in the free DnaA concentration right before the first origin initiates replication [see Figs. 9(a) and 9(b)]. A sharp rise of the initiation potential right before replication initiation is, however, a necessary requirement for synchronous replication initiation. Therefore, the net effect of the initiation cascade on the degree of synchrony is approximately zero and we do not find a significant increase in the degree of synchrony [see Fig. 9(c)].

The datasets generated and analyzed during the current study are available at Zenodo via [50]. The code is publicly available at the Github repository [51] or at Zenodo via [52].

ACKNOWLEDGMENTS

We want to thank Vahe Galstyan for the fruitful discussions and his mathematical insights, and Lorenzo Olivi for inspiring discussions. We acknowledge financial support from The Netherlands Organization of Scientific Research (NWO/OCW) Gravitation program Building a Synthetic Cell (BaSyC) (024.003.019).

APPENDIX A: CELL-CYCLE SIMULATION DETAILS

At every replication initiation event at time t^* a cell division time is set a fixed time $\tau_{\rm div} = t^* + \tau_{\rm cc}$ later. Each set division time $\tau_{\rm div}$ is linked to the chromosome that just initiated replication. When the cell inherits a chromosome that is already being replicated but has not yet reached its division time, it also inherits the next division time (Fig. 10). This method ensures that each daughter cell always obtains a fully replicated chromosome, a necessary requirement for the survival of every cell.

TABLE I. Parameters used in the simulations. One molecule per cubic micrometer corresponds to approximately 1 nM ($1\ \mu\text{m}^{-3} = 1.67$ nM).

Parameter	Name	Value	Motivation
n	Hill coefficient of initiation potential	5	Set to match initiation precision reported in Ref. [2]
v^* (μm^3)	Initiation volume per origin	1	Set to match initiation volume reported in Ref. [2]
m	Hill coefficient of opening probability	10	Ref. [13]
y^*	Critical initiation potential	0.5	Set to maximal sharpness of opening probability
$K_{\rm D}$ (μm^{-3})	Dissociation constant of (de)activators	5	Ref. [22]
$\alpha_{\rm l} l$ ($\mu\text{m}^{-3}\,\text{h}^{-1}$)	Activation rate lipids	LDDR:500, LDDR+titration:800	Set to match initiation volume reported in Ref. [2]
$\beta_{\rm datA}$ (h^{-1})	Deactivation rate *datA*	600	Ref. [15]
$\tau_{\rm datA}$ (h)	Replication time *datA*	0.13	Ref. [15]
f^*	Critical initiator fraction	0.5	Refs. [17,24]
$\tau_{\rm i}$ (h)	Initiation duration	0.27	See Fig. 11
$\alpha_{\rm d1}$ (h^{-1})	Activation rate *DARS1*	100	Refs. [13,16]
$\tau_{\rm d1}$ (h)	Replication time *DARS1*	0.4	Ref. [13]
$\alpha^+_{\rm d2}$ (h^{-1})	High activation rate *DARS2*	600	Combined with $\beta_{\rm rida}$
$\alpha^-_{\rm d2}$ (h^{-1})	Low activation rate *DARS2*	50	Set to arbitrary low value
$\tau_{\rm d2}$ (h)	Replication time *DARS2*	0.25	Ref. [16]
$\tau^+_{\rm d2}$ (h)	Start high activation rate *DARS2*	0.2	Ref. [16]
$\tau^-_{\rm d2}$ (h)	End high activation rate *DARS2*	2/3	Ref. [16]
$\beta_{\rm rida}$ (h^{-1})	Deactivation rate RIDA	500	Refs. [15,31,53]
$[D]_{\rm T}$ (μm^{-3})	Total DnaA concentration	400	Refs. [19,21]
ϕ_0	Gene allocation fraction	4×10^{-4}	Set to match $[D]_{\rm T}$
$K^{\rm s}_{\rm D}$ (μm^{-3})	Dissociation constant of titration sites	1	Ref. [22]
$K^{\rm p}_{\rm D}$	Dissociation constant of promoter	200	Ref. [21,54]
$n^{\rm s}_{\rm ori}$	Number of origin binding sites	10	Ref. [13]
$[D]^*_{\rm ATP,f}$	Critical free ATP-DnaA concentration	10	Ref. [22]
ρ (μm^{-3})	Number density	10^6	Ref. [55]
ϕ_0	Gene allocation fraction	10^{-3}	Ref. [21]
$k^0_{\rm f}$ (s^{-1})	Maximal origin firing rate	1000	Set such that degree of synchrony is maximal
$\tau_{\rm b}$ (h)	Blocking period	0.17	Refs. [27–29]
λ (h^{-1})	Growth rate	1.04	Refs. [2,3]
$T_{\rm C}$ (h)	C-period	2/3	Ref. [8]
$T_{\rm D}$ (h)	D-period	1/3	Ref. [8]

The simulations are performed with a finite-time step δt. Each time step, the volume is updated according to $V(t+\delta t) = V(t) + V(t)\,\lambda\,\delta t$ and the firing rate k_f is evaluated via Eq. (3), i.e., $k_\mathrm{f} = k_\mathrm{f}^0 p_o$, where the opening probability $p_o(y)$ depends on the current initiation potential $y(V)$, which depends on the current volume V of the cell. The firing rate k_f then translates into a probability $0 < (P_\mathrm{fire} = k_\mathrm{f}\delta t) \ll 1$ that during this time step the origin will fire; an origin will then fire when this probability is smaller than a random number ξ, uniformly distributed between 0 and 1, i.e., when $P_\mathrm{fire} < \xi$.

APPENDIX B: COARSE-GRAINED MODEL FOR ORIGIN OPENING

We describe the origin region as a two-state system that can switch between an open (O) or a closed (C) configuration with the opening rate k_o and the closing rate k_c. If the origin is open, replication can be initiated (I) with a maximal firing rate k_f^0:

$$\mathrm{C} \underset{k_\mathrm{c}}{\overset{k_\mathrm{o}}{\rightleftharpoons}} \mathrm{O} \xrightarrow{k_\mathrm{f}^0} \mathrm{I}. \tag{B1}$$

In thermal equilibrium, the ratio of the transition rates between the open and closed states is given by the Boltzmann distribution of the energy difference between the two states:

$$\frac{k_\mathrm{c}}{k_\mathrm{o}} = \frac{e^{-\beta E_\mathrm{c}}}{e^{-\beta E_\mathrm{o}}} = e^{\beta\,\Delta G}, \tag{B2}$$

with $\beta = k_\mathrm{B}\,T$ and the energy difference

$$\Delta G = E_\mathrm{o} - E_\mathrm{c}, \tag{B3}$$

where E_o is the energy of the open state and E_c is the energy of the closed state. The probability to be in the open state as a function of the energy difference ΔG is given by

$$p_\mathrm{o} = \frac{e^{-\beta E_\mathrm{o}}}{e^{-\beta E_\mathrm{o}} + e^{-\beta E_\mathrm{c}}} = \frac{1}{1 + e^{\beta\,\Delta G}}. \tag{B4}$$

Assuming rapid opening and closing dynamics of the origin, the origin firing rate is given by Eq. (3). The higher the initiation potential f in the cell, the more likely is it that the origin is open and that replication can be initiated. We model this observation phenomenologically by assuming that the opening probability p_o increases with the activation potential f following a Hill function [see Eq. (2)].

APPENDIX C: DERIVATION OF APPROXIMATION FOR OPENING PROBABILITY

We want to find an expression for the opening probability p_o and therefore also the instantaneous firing rate k_f [Eq. (3)] as a function of time. We therefore insert Eq. (1) into Eq. (2) to obtain

$$p_\mathrm{o}(f(v)) = \frac{v^{n\,m}}{f^{*m}\,(v^{*n} + v^n)^m + v^{n\,m}} \tag{C1}$$

$$= \frac{v^{n\,m}}{f^{*m}\,v^{*n\,m}\,(1+\tilde{v}^n)^m + v^{n\,m}}, \tag{C2}$$

where we used $\tilde{v} = v/v^*$. According to the binomial formula, we can write

$$(1+\tilde{v}^n)^m = \sum_{k=0}^{m} \binom{m}{k} 1^k\,(\tilde{v}^n)^{m-k} \tag{C3}$$

$$= \sum_{k=0}^{m} \binom{m}{k} (\tilde{v}^n)^{m-k}, \tag{C4}$$

with the binomial coefficient

$$\binom{m}{k} := \frac{m!}{k!\,(m-k)!}. \tag{C5}$$

We introduce the shifted parameter $k' = k - m/2$, such that Eq. (C4) can be rewritten as

$$(1+\tilde{v}^n)^m = \sum_{k'=-m/2}^{m/2} \binom{m}{k' + \frac{m}{2}} (\tilde{v}^n)^{\frac{m}{2}-k'}. \tag{C6}$$

By examining the first and the second terms of the sum in Eq. (C6) separately, we find that the binomial coefficient has a maximum at $k' = 0$ and decays quickly for $k' \neq 0$ [see Fig. 6(a)]. Second, as can be seen in Fig. 6(b), for small $k' \ll \pm m/2$ and sufficiently large Hill coefficient m, the second term is approximately given by

$$\tilde{v}^{n\,(\frac{m}{2}-k')} \approx \tilde{v}^{\frac{mn}{2}}. \tag{C7}$$

Combining these two observations, we can approximate Eq. (C6) by

$$(1+\tilde{v}^n)^m \approx \sum_{k'=-m/2}^{m/2} \binom{m}{k' + \frac{m}{2}} \tilde{v}^{\frac{mn}{2}}. \tag{C8}$$

Finally, using that

$$\sum_{k'=-m/2}^{m/2} \binom{m}{k' + \frac{m}{2}} = 2^m, \tag{C9}$$

we find

$$(1+\tilde{v}^n)^m \approx 2^m\,\tilde{v}^{\frac{mn}{2}}. \tag{C10}$$

Plugging this expression into Eq. (C2) gives

$$p_\mathrm{o}(v) \approx \frac{v^{n\,m}}{f^{*m}\,v^{*n\,m}\,2^m\,\tilde{v}^{\frac{mn}{2}} + v^{n\,m}} \tag{C11}$$

$$= \frac{v^{n\,m}}{f^{*m}\,2^m\,v^{*\frac{nm}{2}}\,v^{\frac{nm}{2}} + v^{n\,m}} \tag{C12}$$

$$= \frac{v^{\frac{nm}{2}}}{f^{*m}\,2^m\,v^{*\frac{nm}{2}} + v^{\frac{nm}{2}}}. \tag{C13}$$

For $f^* = 0.5$ we then find Eq. (5) of the main text with the effective Hill coefficient $n_\mathrm{eff} = n\,m/2$. By comparing the approximation of $p_\mathrm{o}(v)$ in Eq. (5) to a function

$$p_\mathrm{o}^\mathrm{fit}(v) = a^\mathrm{fit}\,\frac{v^{n_\mathrm{eff}^\mathrm{fit}}}{v^{*\,n_\mathrm{eff}^\mathrm{fit}} + v^{n_\mathrm{eff}^\mathrm{fit}}} \tag{C14}$$

that was fitted to $p_\mathrm{o}(f(v))$ [Eq. (C2)], we find that the approximation in Eq. (5) is indeed a good approximation for sufficiently large Hill coefficients n and m, especially at volume close to the critical volume v^* [Fig. 6(c)]. Indeed, the

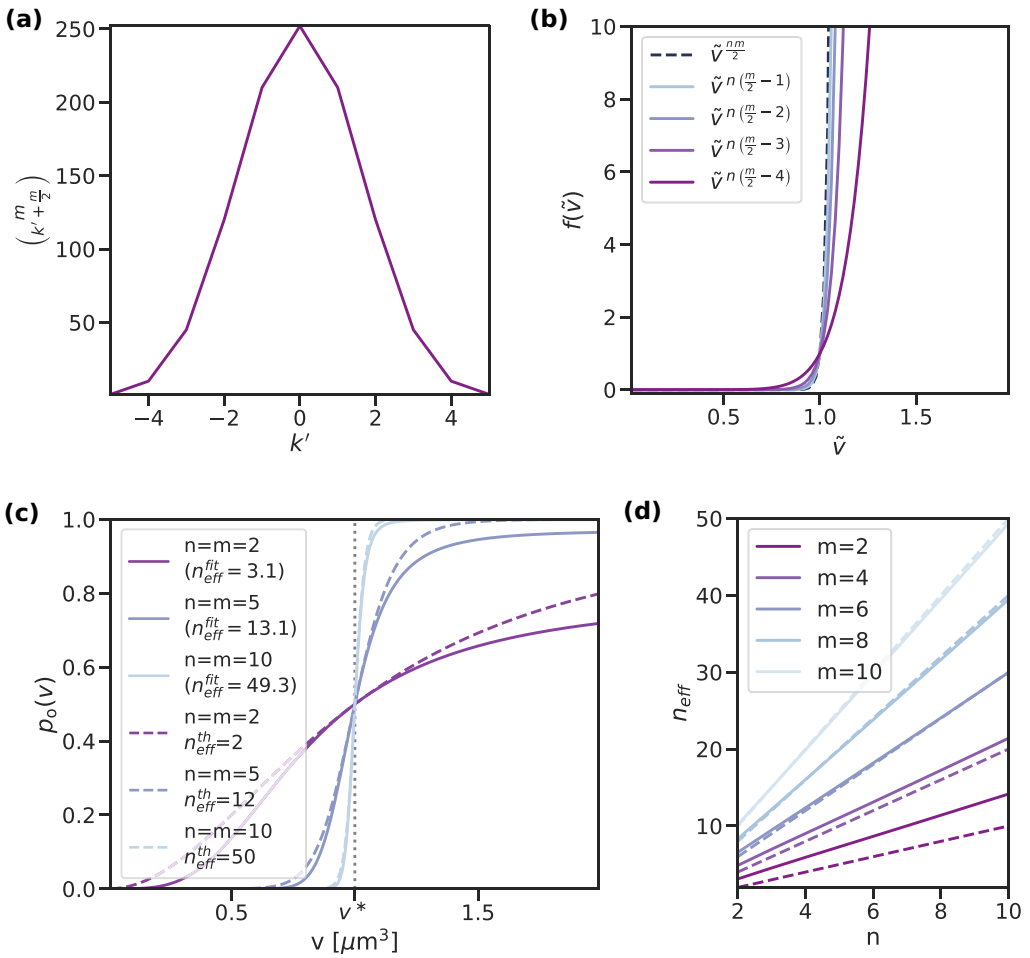

FIG. 6. The instantaneous opening probability can be approximated by a Hill function with an effective Hill coefficient. (a) The binomial coefficient as defined in Eq. (C5) as a function of the index k' for $m = 10$. The binomial coefficient is centered around and maximal at $k' = 0$ and becomes small for $k' \gg 0$. (b) The second term in Eq. (C6) for different values of the index k' as a function of the rescaled volume $\tilde{v} = v/v^*$. For small values of k', the second term in Eq. (C6) is well approximated by the term $\tilde{v}^{\frac{nm}{2}}$ (dashed blue line). (c) The opening probability of the origin $p_o(f(v))$ [Eq. (C2)] as a function of the volume per origin v for different Hill coefficients n and m (solid lines). The effective Hill coefficient $n_{\text{eff}}^{\text{fit}}$ is obtained from a fit of the function $p_o(f(v))$ to a Hill function [Eq. (C14)]. The dashed lines show the approximated opening probability [Eq. (5)] with the effective Hill coefficient as defined in Eq. (6). The vertical dotted line indicates the critical volume per origin, v^*, at which the opening probability equals 1/2. (d) The fitted (solid line) and the approximated [dashed line, Eq. (6)] Hill coefficient as a function of the Hill coefficient n for different values of the Hill coefficient m. Except for very low Hill coefficients n and m, the approximated Hill coefficient agree well. In all graphs $f^* = v^* = 0.5$. (See Table I for all parameters.)

fitted Hill coefficient agrees well with the approximated Hill coefficient in Eq. (6) for a broad range of Hill coefficients n and m, respectively [Fig. 6(d)].

APPENDIX D: PARAMETER CHOICE FOR MAXIMAL FIRING RATE

Combining the approximation for the opening probability as a function of the volume per origin [Eq. (5)], the exponentially growing cell volume $V(t) = V_b\, e^{\lambda t}$, and the expression for the firing rate [Eq. (3)], we find the following time-dependent firing rate of a single origin:

$$k_f(t) = k_f^0 \frac{(V_b\, e^{\lambda t})^{n_{\text{eff}}}}{v^{*\,n_{\text{eff}}} + (V_b\, e^{\lambda t})^{n_{\text{eff}}}}. \tag{D1}$$

From this rate, we can calculate the survival probability

$$S(t) = e^{-\int_{t_0}^{t} dt' k_f(t')} \tag{D2}$$

$$= e^{-\frac{k_f^0}{n_{\text{eff}}\,\lambda} \ln\left(\frac{(V_b e^{\lambda t})^{n_{\text{eff}}} + v^{*\,n_{\text{eff}}}}{V_b^{n_{\text{eff}}} + v^{*\,n_{\text{eff}}}}\right)}, \tag{D3}$$

where we solved the integral with the initial condition $S(t_0 = 0) = 1$. We now impose that at the theoretical initiation volume per origin, $v(t = t^*) = v^*$, the survival probability is exactly $S(t^*) = 0.5$. Using this constraint, we obtain the following expression for the maximal firing rate as a function of the effective Hill coefficient n_{eff}:

$$k_f^0(n_{\text{eff}}) = \frac{n_{\text{eff}}\,\lambda\,\ln(2)}{\ln\left(\frac{2\,v^{*n_{\text{eff}}}}{V_b^{n_{\text{eff}}} + v^{*n_{\text{eff}}}}\right)}. \tag{D4}$$

This parameter choice ensures that the average initiation volume $\langle v^* \rangle$ is given by v^*.

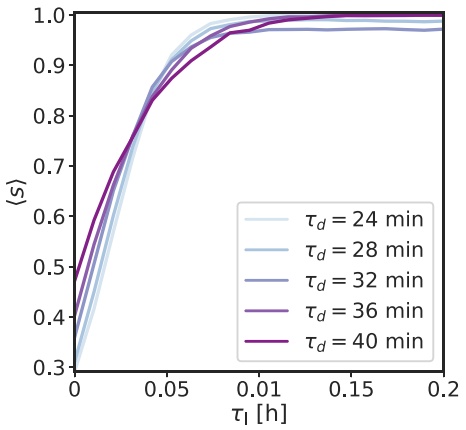

FIG. 7. The average degree of synchrony does not depend strongly on the growth rate of the cell. The average degree of synchrony, $\langle s\rangle$, as a function of the duration of the licensing period τ_l for different cell-doubling times τ_d. The average degree of synchrony, $\langle s\rangle$, is to a good approximation independent of the doubling time τ_d. The small decrease in the degree of synchrony at high licensing times τ_l at a doubling time of $\tau_d = 32$ min is because at this doubling time replication initiation happens almost at the same time as cell division. When the cell divides during an initiation cascade, the number of origins decreases and the counted total number of origins at the end of the cascade is smaller than the total number of origins in both daughter cells. This error in counting the total change in the number of origins, $\Delta n_{\rm ori}$, in Eq. (4) effectively reduces the degree of synchrony, especially for long initiation durations (high licensing times τ_l). The decrease in the minimal average degree of synchrony, $\langle s\rangle$ (at $\tau_l = 0$), with increasing growth rate comes from the overall higher number of origins at higher growth rates and thus a higher denominator in Eq. (4). The effective Hill coefficient is set to $n_{\rm eff} = 50$. (See Table I for all parameters.)

APPENDIX E: DERIVATION OF THE THEORETICAL PREDICTION FOR THE DEGREE OF SYNCHRONY

In the following, we derive a theoretical prediction for the probability that two initiation events happen within a time interval τ_l. We assume here that the two firing events are statistically independent, meaning that between the first initiation event at time t_1 and the time $t_1 + \tau_l$, the change in the number of origins induced by the first event has no effect on the firing of the second event. Using the firing rate in Eq. (D1), we can now calculate the error probability $S_{\rm err}$ that the second event does *not* happen within a time τ_l after the first event, given that the first event happened at time t_1:

$$S_{\rm err}(t_2 - t_1 > \tau_l | t_1) = e^{-\int_{t_1}^{t_1+\tau_l} dt' k_f(t')} \tag{E1}$$

$$= e^{-\frac{k_f^0}{n_{\rm eff}\lambda}\log\left(\frac{(V_b e^{\lambda(t_1+\tau_l)})^{n_{\rm eff}}+v^{*n_{\rm eff}}}{(V_b e^{\lambda t_1})^{n_{\rm eff}}+v^{*n_{\rm eff}}}\right)}. \tag{E2}$$

The average error probability $\langle S_{\rm err}\rangle$ over all initiation times of the first event, t_1, is then given by

$$\langle S_{\rm err}\rangle = \int_0^{\tau_d} dt_1\, q_1(t_1)\, S_{\rm err}(t_2 - t_1 > \tau_l | t_1) \tag{E3}$$

$$= \int_0^{\tau_d} dt_1\, q_1(t_1)\, e^{-\int_{t_1}^{t_1+\tau_l} dt' k_f(t')}, \tag{E4}$$

where τ_d is the doubling time of the cell. The propensity $q_1(t_1)$ that one out of two origin events happens at time t_1 is given by

$$q_1(t_1) = 2\, k_f(t_1)\, e^{-\int_{t_0}^{t_1} dt' 2\, k_f(t')}. \tag{E5}$$

Therefore, the average error probability $\langle S_{\rm err}\rangle$ that the second origin fires after a time τ_l after the first event is given by plugging expression (E5) into Eq. (E4):

$$\langle S_{\rm err}\rangle = 2\int_0^{\tau_d} dt_1\, k_f(t_1)\, e^{-2\int_{t_0}^{t_1} dt' k_f(t')}\, e^{-\int_{t_1}^{t_1+\tau_l} dt' k_f(t')} \tag{E6}$$

$$= 2\,k_f^0 \int_0^{\tau_d} dt_1\, \frac{(V_b\, e^{\lambda t_1})^{n_{\rm eff}}}{v^{*n_{\rm eff}} + (V_b\, e^{\lambda t_1})^{n_{\rm eff}}} \times e^{-\frac{2k_f^0}{n_{\rm eff}\lambda}\ln\left(\frac{(V_b e^{\lambda t_1})^{n_{\rm eff}}+v^{*n_{\rm eff}}}{V_b^{n_{\rm eff}}+v^{*n_{\rm eff}}}\right)} e^{-\frac{k_f^0}{n_{\rm eff}\lambda}\ln\left(\frac{(V_b e^{\lambda(t_1+\tau_l)})^{n_{\rm eff}}+v^{*n_{\rm eff}}}{(V_b e^{\lambda t_1})^{n_{\rm eff}}+v^{*n_{\rm eff}}}\right)}, \tag{E7}$$

where τ_d is the average division time of the cell and $\tau_d \gg \tau_l$, such that the probability that both origins have not yet fired at τ_d becomes negligible. The average probability that the second origin fires within a time interval $\Delta t = t_2 - t_1 < \tau_l$ after the first has fired at t_1 is then given by

$$\langle P(\Delta t < \tau_l)\rangle = 1 - \langle S_{\rm err}(\tau_l)\rangle. \tag{E8}$$

We solve the integral in Eq. (E7) numerically and use expression (7) to predict the degree of synchrony for two origins [see Fig. 3(b)].

One can also calculate numerically the degree of synchrony at higher growth rates where there are typically four or more origins per cell at the beginning of an initiation cascade. The probability that none of the $n-1$ origins fires within the time τ_l after the first origin has fired at t_1 is similar to Eq. (E7) and given by

$$\langle S_{\rm err}\rangle = n\int_0^{\tau_d} dt_1\, k_f(t_1)\, e^{-n\int_{t_0}^{t_1} dt' k_f(t')}\, e^{-(n-1)\int_{t_1}^{t_1+\tau_l} dt' k_f(t')}. \tag{E9}$$

This is the probability that, given that the first origin fires at t_1, all $n-1$ other origins fire later than $t_1 + \tau_l$. Importantly, one now also needs to take into account the cases where only one or more origins fire at $t_1 + \tau_l$ and the others fire before. We here do not derive an expression for the scenario $n > 2$.

APPENDIX F: DERIVATION OF THEORETICAL PREDICTION FOR $\langle \Delta t\rangle$ AND THE CV OF THE INITIATION VOLUME

The average time interval between two independent firing events, $\langle \Delta t\rangle$, can be calculated for the approximate opening probability in Eq. (5) via

$$\langle \Delta t\rangle = \int_0^{\tau_d} dt_1 \int_{t_1}^{\tau_d} dt_2\, 2\, k_f(t_1)\, k_f(t_2)\, e^{-2\int_{t_0}^{t_1} dt' k_f(t')} \times e^{-\int_{t_1}^{t_2} dt'' k_f(t'')}. \tag{F1}$$

Solving this integral numerically gives the pink line in Fig. 3(b).

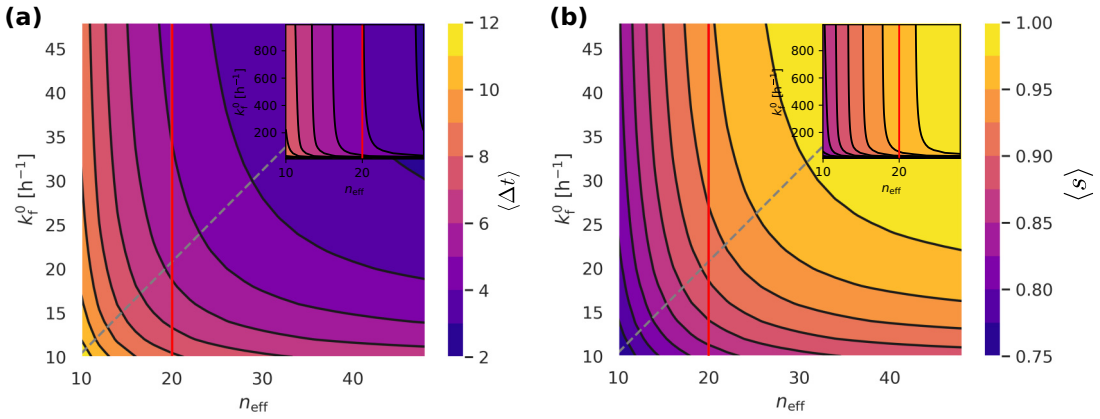

FIG. 8. In the coarse-grained model, the average time interval between the first and the last firing event, $\langle \Delta t \rangle$, and the average degree of synchrony, $\langle s \rangle$, depend both on the effective Hill coefficient n_{eff} and on the maximal firing rate k_f^0. These contour plots show (a) the average time interval between the first and last origin firing event, $\langle \Delta t \rangle$, and (b) the theoretical degree of synchrony, s_{th} [according to Eq. (7)], as a function of the effective Hill coefficient n_{eff} and the maximal firing rate k_f^0 for the licensing period $\tau_l = 9.6$ min $< \tau_b$ at the experimentally observed blocking period of $\tau_b = 10$ min. The dashed gray lines are given by Eq. (D4) and correspond to the parameter choice in the main text where the average initiation volume $\langle v^* \rangle = v^*$ (see Appendix D). For a given Hill coefficient n_{eff} both $\langle \Delta t \rangle$ and $\langle s \rangle$ first increase as a function of the maximal firing rate k_f^0 and then converge to a constant value for higher maximal firing rates. Therefore, at a higher maximal origin firing rate than in Fig. 3(a) the effective Hill coefficient can be lower to achieve the same degree of synchrony. However, panel (a) shows (and the inset more clearly) that there is a minimal n_{eff} necessary to reach the experimentally reported maximal bound on $\langle \Delta t_{\text{expt}}^{\max} \rangle$, corresponding to the limit $k_f^0 \to \infty$. The red vertical lines show that to initiate replication within at least $\langle \Delta t_{\text{expt}}^{\max} \rangle = 4$ min, the minimal Hill coefficient required in the regime of firing rates ($k_f^0 \to \infty$) is $n_{\text{eff}} = 20$. This corresponds to a high degree of synchrony of $s_{\text{th}} \approx 0.96$ (corresponding to $P_s \approx 92\%$) [see panel (b)]. Therefore, the finding of the main text that a high Hill coefficient is required for a high degree of synchrony remains valid. (See Table I for all parameters.)

The theoretical coefficient of variation of the initiation volume V is given by

$$CV = \frac{\sigma}{\mu} = \frac{\sqrt{\langle V^2 \rangle - \langle V \rangle^2}}{\langle V \rangle}, \tag{F2}$$

where we use

$$\langle V \rangle = \int_0^{\tau_d} dt\, k_f(t)\, e^{-\int_{t_0}^{t} dt' k_f(t')}\, V_b\, e^{\lambda t} \tag{F3}$$

and

$$\langle V^2 \rangle = \int_0^{\tau_d} dt\, k_f(t)\, e^{-\int_{t_0}^{t} dt' k_f(t')}\, (V_b\, e^{\lambda t})^2. \tag{F4}$$

In this theoretical model, the only source of noise is intrinsic noise and the CV in Eq. (F2) therefore also corresponds to the intrinsic noise as defined by Ref. [7] based on the derivation of Elowitz *et al.* [56].

APPENDIX G: THE LDDR MODEL

The LDDR model contains all known (de)activators of DnaA with their temporal regulation over the course of the cell cycle: the number of catalytic RIDA complexes is proportional to the number of origins with a rate β_{rida} [31,53] that is only non-zero during the period of active replication T_C. The chromosomal sites *DARS1* and *DARS2* are located near the middle of the chromosome and are replicated at constant times τ_{d1} and τ_{d2}, respectively, after the origin. The activity of *DARS2* is temporally regulated during the cell cycle via binding of the integrating host factor (IHF) [13,16,26]. We model this observation via a step function $\alpha_{d2}(t - t_i)$ that switches to a high value α_{d2}^+ at $t = t_i + \tau_{d2}^+$ and back to a low value α_{d2}^- at $t = t_i + \tau_{d2}^-$ after replication initiation at t_i. *DARS1* activation is modeled via a constant activation rate α_{d1}. We further assume that the concentration of the acidic phospholipids $[l]$ is constant in time and that DnaA is activated by the lipids with a rate α_l. Finally, we assume that every newly synthesized DnaA binds ATP rather than ADP right after synthesis. The change in the ATP-DnaA fraction $f(t)$ in the LDDR model is therefore given by:

$$\begin{aligned} \frac{df}{dt} = &\left(\tilde{\alpha}_l\,[l] + \tilde{\alpha}_{d1}\,[n_{\text{ori}}(t - \tau_{d1})]\right. \\ &\left. + \tilde{\alpha}_{d2}(t)\,[n_{\text{ori}}(t - \tau_{d2})]\right) \frac{1 - f}{\tilde{K}_D + 1 - f} \\ &- \left(\tilde{\beta}_{\text{datA}} + \tilde{\beta}_{\text{rida}}(t)\right)[n_{\text{ori}}]\, \frac{f}{\tilde{K}_D + f} + \lambda\,(1 - f) \end{aligned} \tag{G1}$$

with the re-normalized activation and deactivation rates $\tilde{\alpha}_l = \alpha_l/[D]_T$, $\tilde{\alpha}_{d1} = \alpha_{d1}/[D]_T$, $\tilde{\alpha}_{d2} = \alpha_{d2}/[D]_T$, $\tilde{\beta}_{\text{datA}} = \beta_{\text{datA}}/[D]_T$ and $\tilde{\beta}_{\text{rida}} = \beta_{\text{rida}}/[D]_T$ and the Michaelis-Menten constant $\tilde{K}_D = K_D/[D]_T$. All parameters are described in more detail in our previous paper [25] and their values are listed in Table I.

APPENDIX H: DEFINITION OF THE INITIATION DURATION IN LDDR AND LDDR-TITRATION MODELS

While a synchronization parameter cannot be defined uniquely, we will define one to quantify the degree to which replication is initiated synchronously and then show that the

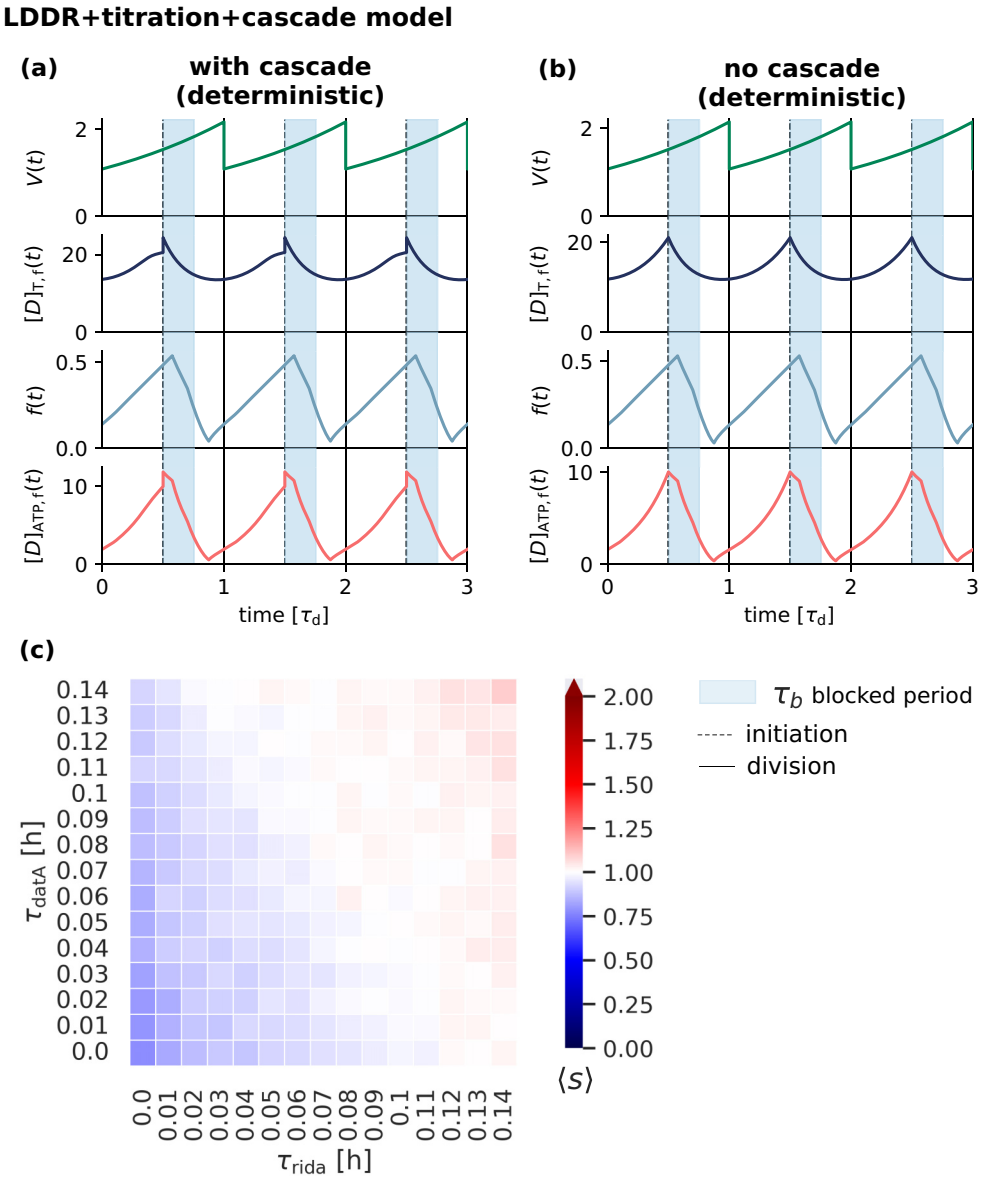

FIG. 9. The initiation cascade does not significantly enhance the degree of synchrony. [(a), (b)] The volume $V(t)$, free DnaA concentration (independent of whether DnaA is bound to ATP or ADP) $[D]_{\mathrm{T,f}}(t)$, the ATP-DnaA fraction $f(t)$, and the free ATP-DnaA concentration $[D]_{\mathrm{ATP,f}}(t)$ as a function of time (in units of the doubling time of the cell, $\tau_{\mathrm{d}} = 0.67$ h $= 40$ min) for a critical free ATP-DnaA concentration of $[D]^{*}_{\mathrm{f,ATP}} = 10\,\mu\mathrm{m}^{-3}$ (a) with and (b) without the initiation cascade. For illustration purposes, replication is here initiated deterministically at all origins as soon as the critical free ATP-DnaA concentration in the cell is reached. (a) When the free ATP-DnaA concentration approaches the critical free ATP-DnaA concentration of $[D]^{*}_{\mathrm{f,ATP}}$, ATP-DnaA proteins begin to bind to the weak, cooperative origin binding sites. This leads to a decrease in the rise of the free DnaA concentration right before replication initiation. Upon replication initiation, the bound ATP-DnaA proteins become unavailable, leading to a sharp increase in the free DnaA concentration. (b) For comparison, we here also show the time traces of a system in which the origin binding sites are not modeled explicitly and the only binding sites are the strong DnaA boxes distributed homogeneously all over the chromosome. (c) The average degree of synchrony, $\langle s \rangle$, as a function of the replication time of the site *datA*, τ_{datA}, and the onset time of RIDA, τ_{rida}, for the same parameters as in Fig. 5(d). Comparing the two panels reveals that the initiation cascade does not significantly enhance the degree of synchrony. For each parameter pair in (c), the average degree of synchrony was obtained from $N = 1000$ consecutive cell cycles. (See Table I for all parameters.)

result is fairly robust to the precise definition. Specifically, the degree of synchrony is obtained by counting the number of origin firing events per initiation event, where the initiation duration τ_{i} is a parameter that we will choose carefully [Fig. 2(a)]. In the coarse-grained model, an initiation event starts when the first origin initiates and ends after the licensing period is over. As after the end of the licensing period the initiation potential drops instantaneously to a very low value, reinitiation events after the end of the licensing period are very unlikely in the coarse-grained model. In the LDDR model, the active fraction f does not, however, decrease instantaneously after RIDA has started and the site *datA* has been doubled [Fig. 4(c)]. Therefore, it is less clear what the initiation period should be. We test the effect of varying the

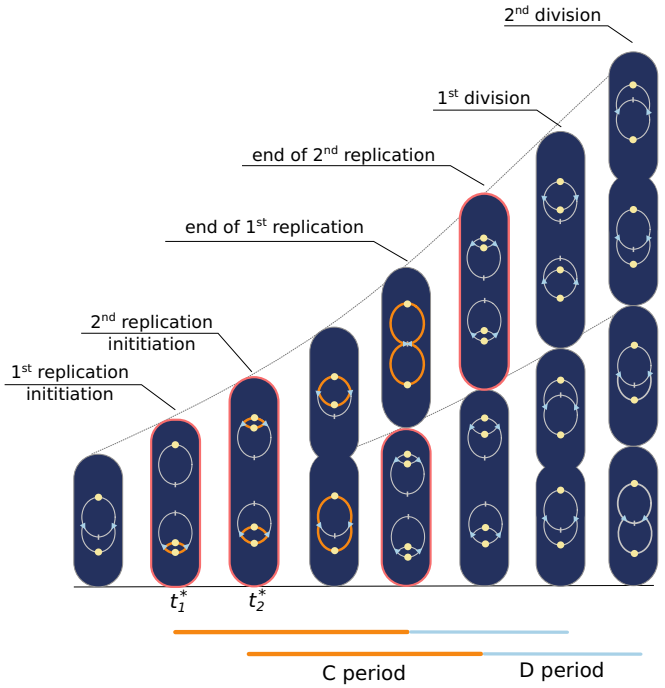

FIG. 10. Scheme of the cell cycle of *E. coli* that shows how each origin firing event triggers cell division a fixed cycling time later. At doubling times that are shorter than the time to replicate the entire chromosome and divide (C+D period), cells are typically born with an ongoing round of chromosomal replication. Here, we illustrate replication initiation in the growth-rate regime with two origins of replication at the beginning of the cell cycle. Replication is initiated stochastically at each origin (yellow circles) at times t_1 and t_2, respectively, and the replication forks (blue triangles) advance towards the terminus (gray bar) with a constant replication speed. In our model, each initiation event triggers cell division a fixed cycling time $\tau_{cc} = T_C + T_D$ after replication has been initiated. This ensures that a cell never divides before the entire chromosome has been replicated. Note that "1st division" ("2nd division") corresponds to the division event triggered by the "1st replication initiation" ("2nd replication initiation") event in the mother cell.

initiation duration τ_i on the average degree of synchrony, $\langle s \rangle$, for different starting times of RIDA, τ_{rida} (Fig. 4). The average degree of synchrony, $\langle s \rangle$, varies strongly with the initiation duration in parameter regimes where replication is initiated asynchronously: at very low starting times of RIDA, τ_{rida}, replication is underinitiated [Fig. 4(b)], but the degree of synchrony nevertheless becomes larger than one at high initiation durations $\tau_i > 0.6\tau_d$ (Fig. 11). The larger the initiation duration τ_i the more origin firing events are counted per initiation event, leading to an average degree of synchrony that is larger than one. Conversely, when the RIDA is starting too late and replication is overinitiated [Fig. 4(b)], the degree of synchrony can nevertheless be smaller than one if the initiation duration is chosen too short. At the optimal starting time of RIDA of $\tau_{rida} = 0.1\,\mathrm{h} \approx 6\,\mathrm{min}$, where replication is initiated synchronously, the choice of the initiation duration becomes, however, less relevant: because all origin firing events happen within a relatively small time window, increasing the initiation duration further does not change the

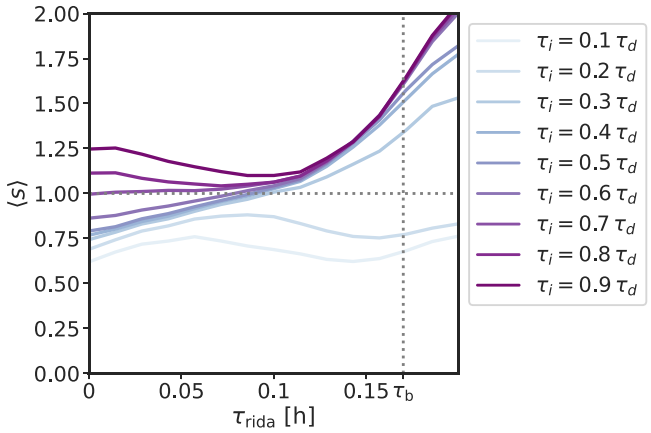

FIG. 11. The average degree of synchrony, $\langle s \rangle$, depends strongly on the initiation duration when replication is initiated asynchronously, but not when replication is initiated synchronously. The average degree of synchrony, $\langle s \rangle$, as a function of the starting time of RIDA, τ_{rida}, for varying initiation durations τ_i (in units of the doubling time τ_d) for the LDDR model. The degree of synchrony s is obtained by counting the number of origin firing events from the first origin firing until the end of the initiation duration τ_i. When replication is initiated synchronously at all origins within a short time interval (at $\tau_{rida} \approx 0.1$ h), the average degree of synchrony does not depend strongly on the initiation period τ_i. When origins are, however, initiated asynchronously over the course of the cell cycle, the average degree of synchrony can either be smaller or larger than one, depending on the duration τ_i. In the rest of this paper, we use an intermediate initiation duration of $\tau_i = 0.4\tau_d$. (See Table I for all parameters.)

degree of synchrony significantly. Only if the initiation duration is chosen way too small ($\tau_i = 0.2\,\tau_d \approx 8\,\mathrm{min}$) or too large ($\tau_i = 0.9\,\tau_d \approx 36\,\mathrm{min}$) does the average degree of synchrony become smaller or larger than one. We therefore in the following choose an intermediate initiation duration of $\tau_i = 0.4\,\tau_d \approx 16\,\mathrm{min}$.

APPENDIX I: THE LDDR-TITRATION MODEL

In the LDDR-titration model, the initiation potential is given by the free ATP-DnaA concentration in the cell. We explicitly model the change in the total number of DnaA proteins N_D^{tot} over the course of the cell cycle as described in Ref. [25], such that the change in copy number N_D^{tot} is given by

$$\frac{dN_D^{tot}}{dt} = \frac{\phi_0\,\rho\,\lambda\,V}{1 + \left(\frac{[D]_{T,f}}{K_D^p}\right)^m} \tag{I1}$$

with gene allocation fraction ϕ_0, number density ρ, growth rate of the cell λ, dissociation constant of the promoter K_D^p, Hill coefficient m and total DnaA concentration in the cytoplasm $[D]_{T,f} = N_D^f/V$. Each chromosome contains a constant number of 300 homogeneously distributed titration sites and the initiator proteins can be either freely diffusing in the cytoplasm or bound to these titration sites with a dissociation constant of K_D^s. As explained in Ref. [25], due to fast binding and unbinding dynamics of the initiator protein to the titration

sites, we assume for simplicity a quasiequilibrium state and use a quadratic equation to calculate at every time step the concentration of initiators $[D]_{\mathrm{T,f}}$ freely diffusing in the cytoplasm. When a new round of DNA replication is initiated, the number of titration sites on that chromosome increases linearly from the moment of initiation of replication t_i until the end of replication at $t_\mathrm{i} + T_\mathrm{C}$.

Using several assumptions that are discussed in detail in Ref. [25], the free ATP-DnaA concentration $[D]_{\mathrm{ATP,f}}$ is then given by the concentration of free DnaA $[D]_{\mathrm{T,f}}$ times the active fraction of DnaA f:

$$[D]_{\mathrm{ATP,f}}(t) = [D]_{\mathrm{T,f}}(t) \times f(t) \tag{I2}$$

APPENDIX J: MODEL FOR THE INITIATION CASCADE

To initiate DNA replication, eight ATP-DnaA proteins and three DnaA proteins independent of the nucleotide-binding state form a cooperative complex at the origin, which induces a conformational change and leads to the opening of the origin [13]. Consequently, the DNA replication machinery binds to the open origin, and replication is initiated. Upon replication initiation, the DnaA proteins that were bound to the origin are likely being released into the cytoplasm, leading to a transient rise in the free DnaA concentration. It has been suggested that the release of origin-bound DnaA proteins from one origin triggers replication initiation at the remaining origins in a so-called initiation cascade [48]. Here we propose a model to test whether the rise in the free DnaA concentration upon replication initiation at one origin could be sufficient to trigger replication initiation at the other origins.

So far, we have modeled the origin opening and firing process in a coarse-grained manner using a Hill function as a function of the initiation potential for the opening probability of the origin (see Appendix B). Now, we instead model the binding of ATP-DnaA to the origin explicitly by introducing weak, cooperative binding sites for ATP-DnaA proteins at the origin. Specifically, we neglect the three strong binding sites to which both ATP- and ADP-DnaA can bind and assume that there are n weak binding sites with the dissociation constant $K_\mathrm{D}^\mathrm{ori}$ to which only ATP-DnaA can bind cooperatively. The probability that n ATP-DnaA proteins are bound to the origin is given by

$$p_\mathrm{b}^\mathrm{n} = \frac{Z_\mathrm{b}^\mathrm{n}}{\sum_{i=0}^{N} Z_\mathrm{i}}, \tag{J1}$$

where Z_b^n is the partition function of n proteins bound to the origin and $\sum_{i=0}^{N} Z_\mathrm{i}$ is the sum over all possible configurations the origin can be in. Let us first consider the scenario of only two cooperative binding sites. This gives rise to the following probability that two ATP-DnaA proteins are bound to the origin:

$$p_\mathrm{b}^2 = \frac{Z_\mathrm{b}^2}{Z_\mathrm{b}^0 + 2\,Z_\mathrm{b}^1 + Z_\mathrm{b}^2}. \tag{J2}$$

The statistical weight of zero bound ATP-DnaA proteins is normalized to one, $Z_\mathrm{b}^0 = 1$, and the weight of one bound ATP-DnaA protein is given by $Z_\mathrm{b}^1 = [D]_{\mathrm{f,ATP}}/K_\mathrm{D}$ with the dissociation constant $K_\mathrm{D} = c_0^{-1}\, e^{-\beta\,\Delta G}$ and the free ATP-DnaA concentration $[D]_{\mathrm{f,ATP}}$. The weight of two bound ATP-DnaA proteins is then given by $Z_\mathrm{b}^2 = w\,[D]_{\mathrm{f,ATP}}^2/K_\mathrm{D}^2$, where $w = e^{\beta\,\Delta E}$ accounts for the additional energy gain from cooperative binding of two ATP-DnaA proteins. When cooperative binding is very strong then $\Delta E \gg \Delta G$ and we can neglect terms with lower powers of w:

$$p_\mathrm{b}^2 \approx \frac{Z_\mathrm{b}^2}{Z_\mathrm{b}^0 + Z_\mathrm{b}^2} = \frac{w\,[D]_{\mathrm{f,ATP}}^2/K_\mathrm{D}^2}{1 + w\,[D]_{\mathrm{f,ATP}}^2/K_\mathrm{D}^2} = \frac{[D]_{\mathrm{f,ATP}}^2}{\left(\frac{K_\mathrm{D}}{\sqrt{w}}\right)^2 + [D]_{\mathrm{f,ATP}}^2}. \tag{J3}$$

This expression can be generalized to the case of n strongly cooperative ATP-DnaA origin binding sites:

$$p_\mathrm{b}^\mathrm{n} \approx \frac{[D]_{\mathrm{f,ATP}}^n}{\left(\frac{K_\mathrm{D}}{\sqrt[n]{w}}\right)^n + [D]_{\mathrm{f,ATP}}^n}. \tag{J4}$$

We therefore recover expression (2) for the origin opening probability in the coarse-grained model where now the critical free ATP-DnaA concentration is given by $[D]_{\mathrm{ATP,f}}^* = K_\mathrm{D}/\sqrt[n]{w}$.

In order to calculate the free DnaA concentration $[D]_\mathrm{f}$ in the scenario where both DnaA forms can bind to the 300 homogeneously distributed strong binding sites on the chromosome and ATP-DnaA can additionally bind cooperatively to n weak binding sites on the origin, we write down the following expression:

$$[D]_\mathrm{f} = [D]_\mathrm{T} - [D]_\mathrm{s} - [D]_\mathrm{o}, \tag{J5}$$

where $[D]_\mathrm{T}$ is the total DnaA concentration in the cell, $[D]_\mathrm{s}$ is the concentration of titration-site bound DnaA, and $[D]_\mathrm{o}$ is the origin-bound concentration of ATP-DnaA. An expression for the titration-site bound concentration $[D]_\mathrm{s}$ as a function of the free DnaA concentration $[D]_\mathrm{f}$ is obtained from the quasiequilibrium approximation as explained in Ref. [25],

$$[D]_\mathrm{s} = \frac{[s]_\mathrm{T}\,[D]_\mathrm{f}}{K_\mathrm{D}^\mathrm{s} + [D]_\mathrm{f}}, \tag{J6}$$

with the total titration site concentration $[s]_\mathrm{T}$ and the dissociation concentration of the titration sites K_D^s. The origin-bound ATP-DnaA concentration $[D]_\mathrm{o}$ is given by the probability p_b^n that n ATP-DnaA proteins are bound to the origin times the total concentration of proteins that can be bound to these origin sites. This total concentration is given by the concentration of origins that are available for ATP-DnaA binding $[n_\mathrm{ori}^\mathrm{f}]$ times the number of binding sites per origin, n. Therefore, we obtain the following expression for the free DnaA concentration:

$$[D]_\mathrm{f} = [D]_\mathrm{T} - \frac{[s]_\mathrm{T}\,[D]_\mathrm{f}}{K_\mathrm{D}^\mathrm{s} + [D]_\mathrm{f}} - \frac{n\left[n_\mathrm{ori}^\mathrm{f}\right]([D]_\mathrm{f}\,f)^n}{\left(\frac{K_\mathrm{D}}{\sqrt[n]{w}}\right)^n + ([D]_\mathrm{f}\,f)^n}. \tag{J7}$$

We here made the simplifying assumption that the free ATP-DnaA concentration $[D]_{\mathrm{f,ATP}}$ is given by the ATP-DnaA fraction f times the free DnaA concentration $[D]_\mathrm{f}$. This is a reasonable approximation because the number of origin binding sites is small compared to the total number of DnaA proteins and the total number of titration sites. The total fraction of ATP-DnaA proteins in the cell f is therefore approximately equal to the fraction of ATP-DnaA proteins in the cytoplasm. Importantly, as explained in Ref. [25], we assume that the switch components (de)activate DnaA independent of whether it is bound to the chromosome (either titration sites

or origin sites) or freely diffusing in the cytoplasm. We solve Eq. (J7) numerically at every time step of the simulations given the total titration site concentration $[s]_T$, the total DnaA concentration $[D]_T$, and the total number of ATP-DnaA available origin binding sites $[n^f_{ori}]$. Replication is again initiated stochastically at every origin with a rate $k_f = k^0_f\, p^n_b$. We model the effect that DnaA proteins are released to the cytoplasm upon replication initiation by transiently reducing the number of available origin binding sites for a duration of $\tau_b = 10$ min after an origin has initiated replication.

Modeling the ATP-DnaA binding to the origins explicitly does not significantly increase the degree of synchrony for a broad range of parameters. When the free ATP-DnaA concentration rises and approaches the critical free ATP-DnaA concentration $[D]^*_{ATP,f}$, ATP-DnaA begins to bind cooperatively to the origin binding sites. This causes a weaker rise in the free DnaA concentration right before replication initiation as compared to a system without these origin binding sites [Figs. 9(a) and 9(b)]. After an origin has been initiated, the origin binding sites become unavailable, causing an increase in the free DnaA concentration after replication initiation [Figs. 9(a) and 9(b)]. While this increase should enhance the probability of other origins to fire replication as well, the weaker rise in the free concentration before replication initiation reduces the sharpness of the rise in the free ATP-DnaA concentration and should therefore lead to a decrease in the degree of synchrony. Indeed, comparing the simulations in which the origin binding is modeled explicitly [Fig. 9(c)] to the previous model in which we simply used a Hill function for the opening probability [Fig. 5(d)] shows that the degree of synchrony is not significantly enhanced by the initiation cascade. The reason likely is that the positive effect of the initiation cascade is counterbalanced by the negative effect of a lower rise in the free concentration before replication initiation.

[1] I. H. Jain, V. Vijayan, and E. K. O'Shea, Spatial ordering of chromosomes enhances the fidelity of chromosome partitioning in cyanobacteria, Proc. Natl. Acad. Sci. USA **109**, 13638 (2012).

[2] M. Wallden, D. Fange, E. G. Lundius, Ö. Baltekin, and J. Elf, The synchronization of replication and division cycles in individual *E. coli* cells, Cell **166**, 729 (2016).

[3] F. Si, D. Li, S. E. Cox, J. T. Sauls, O. Azizi, C. Sou, A. B. Schwartz, M. J. Erickstad, Y. Jun, X. Li, and S. Jun, Invariance of initiation mass and predictability of cell size in *Escherichia coli*, Curr. Biol. **27**, 1278 (2017).

[4] J. T. Sauls, S. E. Cox, Q. Do, V. Castillo, Z. Ghulam-Jelani, and S. Jun, Control of *Bacillus subtilis* replication initiation during physiological transitions and perturbations, mBio **10**, e02205 (2019).

[5] I. Santi, N. Dhar, D. Bousbaine, Y. Wakamoto, and J. D. McKinney, Single-cell dynamics of the chromosome replication and cell division cycles in mycobacteria, Nat. Commun. **4**, 2470 (2013).

[6] E. S. Egan, A. Løbner-Olesen, and M. K. Waldor, Synchronous replication initiation of the two *Vibrio cholerae* chromosomes, Curr. Biol. **14**, R501 (2004).

[7] T. Boesen, G. Charbon, H. Fu, C. Jensen, D. Li, S. Jun, and A. Lobner-Olesen, Robust control of replication initiation in the absence of DnaA-ATP $\leftrightharpoons$ DnaA-ADP regulatory elements in *Escherichia coli*, bioRxiv:2022.09.08.507175 (2022).

[8] S. Cooper and C. E. Helmstetter, Chromosome replication and the division cycle of *Escherichia coli* Br, J. Mol. Biol. **31**, 519 (1968).

[9] K. Skarstad, E. Boye, and H. B. Steen, Timing of initiation of chromosome replication in individual *Escherichia coli* cells. EMBO J. **5**, 1711 (1986).

[10] F. G. Hansen, B. B. Christensen, and T. Atlung, The initiator titration model: Computer simulation of chromosome and minichromosome control, Res. Microbiol. **142**, 161 (1991).

[11] F. G. Hansen and T. Atlung, The DnaA tale, Front. Microbiol. **9**, 1 (2018).

[12] T. Katayama, S. Ozaki, K. Keyamura, and K. Fujimitsu, Regulation of the replication cycle: Conserved and diverse regulatory systems for DnaA and oriC, Nat. Rev. Microbiol. **8**, 163 (2010).

[13] T. Katayama, K. Kasho, and H. Kawakami, The DnaA cycle in *Escherichia coli*: Activation, function and inactivation of the initiator protein, Front. Microbiol. **8**, 1 (2017).

[14] L. Dewachter, N. Verstraeten, M. Fauvart, and J. Michiels, An integrative view of cell cycle control in *Escherichia coli*, FEMS Microbiol. Rev. **42**, 116 (2018).

[15] K. Kasho and T. Katayama, DnaA binding locus datA promotes DnaA-ATP hydrolysis to enable cell cycle-coordinated replication initiation, Proc. Natl. Acad. Sci. USA **110**, 936 (2013).

[16] K. Kasho, K. Fujimitsu, T. Matoba, T. Oshima, and T. Katayama, Timely binding of IHF and Fis to DARS2 regulates ATP-DnaA production and replication initiation, Nucleic Acids Res. **42**, 13134 (2014).

[17] K. Kurokawa, S. Nishida, A. Emoto, K. Sekimizu, and T. Katayama, Replication cycle-coordinated change of the adenine nucleotide-bound forms of DnaA protein in *Escherichia coli*, EMBO J. **18**, 6642 (1999).

[18] S. Nishida, K. Fujimitsu, K. Sekimizu, T. Ohmura, T. Ueda, and T. Katayama, A nucleotide switch in the *Escherichia coli* DnaA protein initiates chromosomal replication, J. Biol. Chem. **277**, 14986 (2002).

[19] C. Speck and W. Messer, Mechanism of origin unwinding: Sequential binding of DnaA to double- and single-stranded DNA, EMBO J. **20**, 1469 (2001).

[20] K. Keyamura, Y. Abe, M. Higashi, T. Ueda, and T. Katayama, DiaA dynamics are coupled with changes in initial origin complexes leading to helicase loading, J. Biol. Chem. **284**, 25038 (2009).

[21] F. G. Hansen, T. Atlung, R. E. Braun, A. Wright, P. Hughes, and M. Kohiyama, Initiator (DnaA) protein concentration as a function of growth rate in *Escherichia coli* and *Salmonella typhimurium*, J. Bacteriol. **173**, 5194 (1991).

[22] S. Schaper and W. Messer, Interaction of the initiator protein DnaA of *Escherichia coli* with its DNA target, J. Biol. Chem. **270**, 17622 (1995).

[23] K. Fujimitsu, T. Senriuchi, and T. Katayama, Specific genomic sequences of *E. coli* promote replicational initiation by directly reactivating ADP-DnaA, Genes Dev. **23**, 1221 (2009).

[24] T. Katayama, K. Fujimitsu, and T. Ogawa, Multiple pathways regulating DnaA function in *Escherichia coli*: Distinct roles for DnaA titration by the datA locus and the regulatory inactivation of DnaA, Biochimie **83**, 13 (2001).

[25] M. Berger and P. R. ten Wolde, Robust replication initiation from coupled homeostatic mechanisms, Nat. Commun. **13**, 6556 (2022).

[26] L. Riber, J. Frimodt-Møller, G. Charbon, and A. Løbner-Olesen, Multiple DNA binding proteins contribute to timing of chromosome replication in *E. coli*, Front. Mol. Biosci. **3**, 1 (2016).

[27] J. L. Campbell and N. Kleckner, *E. coli* oriC and the dnaA gene promoter are sequestered from dam methyltransferase following the passage of the chromosomal replication fork, Cell **62**, 967 (1990).

[28] M. Lu, J. L. Campbell, E. Boye, and N. Kleckner, SeqA: A negative modulator of replication initiation in *E. coli*, Cell **77**, 413 (1994).

[29] T. Waldminghaus and K. Skarstad, The *Escherichia coli* SeqA protein, Plasmid **61**, 141 (2009).

[30] J. I. Kato and T. Katayama, Hda, a novel DnaA-related protein, regulates the replication cycle in *Escherichia coli*, EMBO J. **20**, 4253 (2001).

[31] K. Nakamura and T. Katayama, Novel essential residues of Hda for interaction with DnaA in the regulatory inactivation of DnaA: Unique roles for Hda AAA^+ Box VI and VII motifs, Mol. Microbiol. **76**, 302 (2010).

[32] R. Kitagawa, H. Mitsuki, T. Okazaki, and T. Ogawa, A novel DnaA protein-binding site at 94.7 min on the *Escherichia coli* chromosome, Mol. Microbiol. **19**, 1137 (1996).

[33] R. Kitagawa, T. Ozaki, S. Moriya, and T. Ogawa, Negative control of replication initiation by a novel chromosomal locus exhibiting exceptional affinity for *Escherichia coli* DnaA protein, Genes Dev. **12**, 3032 (1998).

[34] T. Ogawa, Y. Yamada, T. Kuroda, T. Kishi, and S. Moriya, The datA locus predominantly contributes to the initiator titration mechanism in the control of replication initiation in *Escherichia coli*, Mol. Microbiol. **44**, 1367 (2002).

[35] S. Nozaki, Y. Yamada, and T. Ogawa, Initiator titration complex formed at datA with the aid of IHF regulates replication timing in *Escherichia coli*, Genes Cells **14**, 329 (2009).

[36] W. D. Donachie, Relationship between cell size and time of initiation of DNA replication, Nature (London) **219**, 1077 (1968).

[37] F. Si, G. Le Treut, J. T. Sauls, S. Vadia, P. A. Levin, and S. Jun, Mechanistic origin of cell-size control and homeostasis in bacteria, Curr. Biol. **29**, 1760 (2019).

[38] G. Witz, E. van Nimwegen, and T. Julou, Initiation of chromosome replication controls both division and replication cycles in *E. coli* through a double-adder mechanism, eLife **8**, e48063 (2019).

[39] N. E. Buchler and M. Louis, Molecular titration and ultrasensitivity in regulatory networks, J. Mol. Biol. **384**, 1106 (2008).

[40] A. Goldbeter and D. E. Koshland, An amplified sensitivity arising from covalent modification in biological systems, Proc. Natl. Acad. Sci. USA **78**, 6840 (1981).

[41] T. Katayama, T. Kubota, K. Kurokawa, E. Crooke, and K. Sekimizu, The initiator function of DnaA protein is negatively regulated by the sliding clamp of the *E. coli* chromosomal replicase, Cell **94**, 61 (1998).

[42] J. Elf, G.-W. Li, and X. S. Xie, Probing transcription factor dynamics at the single-molecule level in a living cell, Science **316**, 1191 (2007).

[43] T. Bach, M. A. Krekling, and K. Skarstad, Excess SeqA prolongs sequestration of oriC and delays nucleoid segregation and cell division, EMBO J. **22**, 315 (2003).

[44] G. Charbon, L. Riber, M. Cohen, O. Skovgaard, K. Fujimitsu, T. Katayama, and A. Løbner-Olesen, Suppressors of $DnaA^{ATP}$ imposed overinitiation in *Escherichia coli*, Mol. Microbiol. **79**, 914 (2011).

[45] E. Boye and A. Løbner-Olesen, The role of dam methyltransferase in the control of DNA replication in *E. coli*, Cell **62**, 981 (1990).

[46] U. Von Freiesleben, M. A. Krekling, F. G. Hansen, and A. Løbner-Olesen, The eclipse period of *Escherichia coli*, EMBO J. **19**, 6240 (2000).

[47] D. S. Hwang, E. Crooke, and A. Kornberg, Aggregated dnaA protein is dissociated and activated for DNA replication by phospholipase or dnaK protein, J. Biol. Chem. **265**, 19244 (1990).

[48] A. Løbner-Olesen, F. G. Hansen, K. V. Rasmussen, B. Martin, and P. L. Kuempel, The initiation cascade for chromosome replication in wild-type and Dam methyltransferase deficient *Escherichia coli* cells, EMBO J. **13**, 1856 (1994).

[49] J. Herrick, M. Kohiyama, T. Atlung, and F. G. Hansen, The initiation mess? Mol. Microbiol. **19**, 659 (1996).

[50] https://doi.org/10.5281/zenodo.8177184.

[51] https://github.com/MareikeBerger/Synchrony/.

[52] https://doi.org/10.5281/zenodo.8177164.

[53] M. C. Moolman, S. T. Krishnan, J. W. J. Kerssemakers, A. van den Berg, P. Tulinski, M. Depken, R. Reyes-Lamothe, D. J. Sherratt, and N. H. Dekker, Slow unloading leads to DNA-bound β_2-sliding clamp accumulation in live *Escherichia coli* cells, Nat. Commun. **5**, 5820 (2014).

[54] C. Speck, C. Weigel, and W. Messer, ATP- and ADP-DnaA protein, a molecular switch in gene regulation, EMBO J. **18**, 6169 (1999).

[55] R. Milo, What is the total number of protein molecules per cell volume? A call to rethink some published values, BioEssays **35**, 1050 (2013).

[56] M. B. Elowitz, A. J. Levine, E. D. Siggia, and P. S. Swain, Stochastic gene expression in a single cell, Science **297**, 1183 (2002).